Published in final edited form as:
J Am Chem Soc. 2010 November 10; 132(44): 15610–15623. doi:10.1021/ja105855v.

1,4-Addition of Lithium Diisopropylamide to Unsaturated Esters: Role of Rate-Limiting Deaggregation, Autocatalysis, Lithium Chloride Catalysis and Other Mixed Aggregation Effects

Yun Ma, **Alexander C. Hoepker**, **Lekha Gupta**, **Marc F. Faggin**, and **David B. Collum***
Department of Chemistry and Chemical Biology, Baker Laboratory, Cornell University, Ithaca, New York 14853-1301

Abstract

Lithium diisopropylamide (LDA) in tetrahydrofuran at −78 °C undergoes 1,4-addition to an unsaturated ester via a rate-limiting deaggregation of LDA dimer followed by a post-rate-limiting reaction with the substrate. Muted autocatalysis is traced to a lithium enolate-mediated deaggregation of the LDA dimer and the intervention of LDA-lithium enolate mixed aggregates displaying higher reactivities than LDA. Striking accelerations are elicited by <1.0 mol % LiCl. Rate and mechanistic studies reveal that the uncatalyzed and catalyzed pathways funnel through a common monosolvated-monomer-based intermediate. Four distinct classes of mixed aggregation effects are discussed.

Introduction

1,4-Additions of lithium amides have been reported on numerous occasions.[1−3] In one of the earliest reports, Schlessinger and co-workers found that attempted enolizations of unsaturated esters using lithium diisopropylamide (LDA) in tetrahydrofuran (THF) at −78 °C afforded β-amino esters instead.[1,4] They solved the problem by adding hexamethylphosphoramide (HMPA). Davies and coworkers, recognizing the medicinal importance of β-amino esters, developed highly enantioselective 1,4-additions of structurally analogous β-phenethylamine-derived lithium dialkylamides.[3]

Our interest was piqued by the 1,4-addition of LDA described in eq 1. Previous studies of the 1,4-addition in the presence of HMPA show that addition occurs to the exclusion of enolization via highly solvated LDA dimers suggested to be triple ions.[5−7] When the reaction is carried out in the absence of HMPA under conditions that would be familiar to synthetic organic chemists—LDA/THF/−78 °C—strange decays are observed that are neither first nor second order (Figure 1, curve A). The near linearity of these decays seems more akin to a zeroth-order dependence on ester.[8,9] Moreover, traces of LiCl (<1 mol %) elicit a 70-fold acceleration accompanied by curvature that appears decidedly more normal (Figure 1, inset).

dbc6@cornell.edu.

Supporting Information. NMR, rate, and computational data, experimental protocols, details on the numeric integrations, and a complete list of authors for reference 25 (42 pages). This material is available free of charge via the Internet at http://pubs.acs.org.

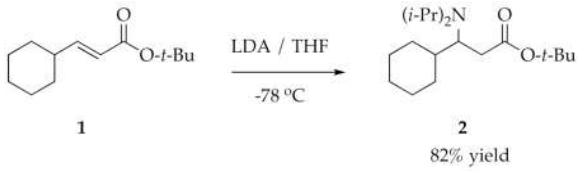

1 2 82% yield

(1)

We describe herein rate and mechanistic studies of the 1,4-addition in eq 1. Superposition of rate-limiting deaggregation, intervention of LDA-lithium enolate mixed aggregates causing muted autocatalysis, and marked catalysis by LiCl present considerable mechanistic complexity.10 Such overt complexity is exhilarating in a mechanistic context, yet the growing number of examples of such odd effects affiliated with LDA/THF/−78 °C are troubling in light of the prevalence of these conditions in organic synthesis.11,12 Furthermore, the LiCl catalysis—a catalysis detectable using as little as 1.0 ppm LiCl—represents a mixed aggregation effect that is, to the best of our knowledge, undocumented.13−15

The results section describes strategies and tactics for specialists who wish to understand the details of the rate studies; the section culminates in a mechanistic hypothesis that accounts for the disparate behaviors. The discussion section summarizes the results for a more general audience and describes how mixed aggregates influence reactivity.

Results

Caveat: Purification of LDA

We previously showed by potentiometry16 and ion chromatography17 that recrystallized LDA18 prepared from recrystallized *n*-BuLi19 contains <0.02 mol % LiCl.11 Accelerations of the 1,4-addition in eq 1 by as little as *0.001 mol % LiCl*, however, prompted us to modify a literature synthesis20 of rigorously LiCl-free LDA from lithium metal, diisopropylamine, isoprene, and dimethylethylamine (DMEA). DMEA accelerates the reduction yet does not remain bound to recrystallized LDA.21 Despite taking these precautions, however, we have observed some variability from stock solutions prepared from a common batch of LDA. Control experiments examining the influence of LDA aging, traces of H_2O and O_2, contaminants in solvents, joint greases, and even the specific researcher carrying out the work failed to uncover the source of this residual variability. The consequences were not large, although triplicate measurements proved necessary in some instances.

Solution Structures

Reaction of 2.0 equiv of LDA with unsaturated ester **1** in THF at −78 °C with slow warming to room temperature affords β-amino ester **2** in 82% yield (eq 1).5 Monitoring the reaction of [^{6}Li,^{15}N]LDA with ester **1** using ^{6}Li and ^{15}N NMR spectroscopy reveals LDA-lithium enolate mixed dimer **4** along with a concentration-independent pair of resonances in nearly 1:1 ratio shown by the absence of ^{6}Li-^{15}N coupling to be enolate **5** (Figure 2). Although tempted to presume that the two resonances derived from an *E/Z* mixture, we suspected that they were homochiral and heterochiral dimers **5a**. (The existence of chelation is depicted out of convenience; the typically small Li-N coupling anticipated for an Li-NR_3 interaction22 is not observed.) By varying the proportions of LDA and lithium enolate and monitoring LDA homodimer **3**, mixed dimer **4**, and the enolate homoaggregates—an A_2-AE-E_n ensemble—we used the method of continuous variation (the method of Job23) to show that the enolate (E_n) is indeed a dimer (Figure 3). Detailed descriptions of this method for characterizing

lithium enolates have been described.24 Although monomeric enolate is not observed, it is invoked as a fleeting intermediate. Density functional theory (DFT) computations at the B3LYP/6–31G(d) level25 of theory suggest disolvated monomer **5b** as the fleetingly stable resting state.

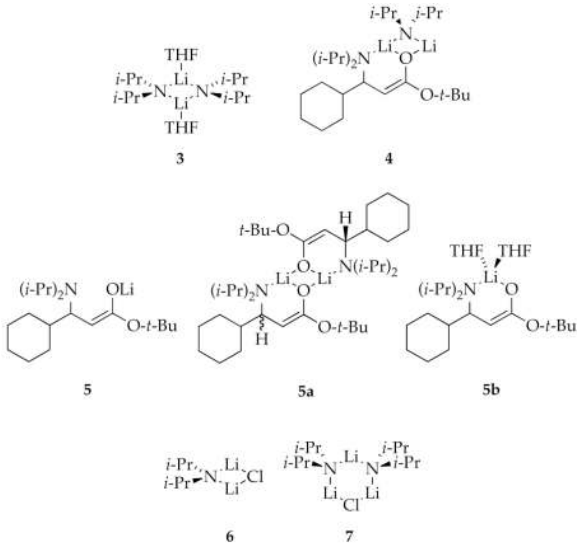

Catalysis by LiCl is discussed in light of the structures of LDA-LiCl mixed aggregates. Previous studies showed LiCl to be dimeric in THF solution.26,27 Mixtures of LDA with very low LiCl concentrations used in the rate studies described below (≤2 mol % LiCl) afford a LiCl-concentration-independent 1:8 mixture of **6** and **7** to the exclusion of free LiCl.27,28

Kinetics: General Protocols

LDA used in rate studies was prepared as described above. Exogenous LiCl was generated in situ from $Et_3N{\cdot}HCl$.29 (The Et_3N by-product is a poor ligand21 that has no effect on LDA structure or reactivity.) The disappearance of ester **1** (1715 cm^{-1}) during the 1,4-additions was monitored using in situ IR spectroscopy.30 Formation of lithium enolate **5** (1630 cm^{-1}) correlates with the loss of **1**. Note, however, that the absorbance at 1630 cm^{-1} arises from the superposition of mixed and homoaggregated dimers **4** and **5a**, respectively. Using ^{6}Li NMR spectroscopy we show that this IR spectral simplicity belies a substantial underlying complexity (vide infra).31

Strange Curvatures

Monitoring additions of LDA to ester **1** by IR spectroscopy under pseudo-first-order conditions (excess LDA) shows a linear decay, suggesting a zeroth-order dependence on ester **1**. Equimolar mixtures of LDA and ester **1** (second-order conditions) afford the decay depicted in Figure 4. If the linearity in Figure 1 derived solely from a zeroth-order in ester **1**, the zeroth-order dependence in conjunction with a first-order LDA dependence would cause the decay in Figure 4 to be overall first order. The first-order fit in Figure 4 (dashed line) is poor, suggesting a persistent linearity stemming from autocatalysis (vide infra). (Previous studies of arylcarbamate lithiations revealed linear decays that were traced to straightening of first-order decays by autocatalysis.11)

^{6}Li NMR spectroscopy allows us to follow the loss of LDA dimer **3**, mixed dimer **4**, and enolate dimer **5a** (Figure 5). The concentrations of the aggregates also allow us to calculate

the concentration of the spectroscopically silent ester **1**. The calculated linear decay of ester **1** correlates well with the experimentally measured linear decay detected by IR spectroscopy. The curved loss of LDA dimer **3**—the noncorrelation with the ester—reflects the consumption of **3** both by metalation and formation of mixed dimer **4**. The time dependencies of **4** and **5a** (represented as A_2 and AE in Figures 5–8) clearly depart from conventional behavior. Minor changes in initial ester concentration produce overt visual changes (Figure 6). Even more striking curvatures and discontinuities are observed using *n*-alkyl ester **12** (Figures 7 and 8). (Ester **12**, *n*-$C_7H_{15}CH{=}CHCO_2$-*t*-Bu, is introduced in the context of competition studies below.) The overshoot of the concentration of enolate dimer **5a** relative to the final equilibrium value and the discontinuity in the mixed dimer concentration place significant constraints on a mechanistic model. Rate studies described below extract the critical details required to account for the strange time-dependent concentrations, and best-fit numerical integrations afford the curves (vide infra).

Kinetics: Uncatalyzed 1,4-Additions

The mechanism of the uncatalyzed 1,4-addition—the addition before the appearance of mixed dimers and onset of autocatalysis—was examined by monitoring the rates at early conversion using IR spectroscopy. A plot of ester concentrations versus time at differing initial concentrations of ester **1** (Figure 9) shows linear, parallel decays consistent with a zeroth-order dependence, which is confirmed by a plot of the initial rates versus initial ester concentration (Figure 10). Plots of initial rates versus LDA concentration (Figure 11)32 and THF concentration (Figure 12) reveal first-order dependencies in both instances. The idealized33 rate law (eq 2) is consistent with a rate-limiting deaggregation (eq 3) followed by a post-rate-limiting reaction with ester **1**.34 To describe some fairly complex mechanistic scenarios, we take the liberty to introduce the following shorthand: A = an LDA monomeric subunit and S = THF (e.g., A_2S_2 = **3**).

$$-d[\mathbf{1}]/dt = k[A_2S_2][S] \tag{2}$$

$$A_2S_2 + S \xrightarrow{k} [A_2S_3]^{\ddagger} \tag{3}$$

DFT computations show that trisolvated-dimer-based transition structures representing rate-limiting open dimer formation (**8**) and deaggregation (**9**) are both plausible (Scheme 1).35 The dimer-based rate-limiting step does *not* attest to whether the post-rate-limiting 1,4-addition is monomer or dimer based, but strong support for a monomer-based 1,4-addition emerges from studies of catalysis (vide infra).

Autocatalysis

Product-derived acceleration—so-called autocatalysis—in its most extreme form manifests sigmoidal decays of substrate versus time36·37 and should be most easily observed using equimolar mixtures of LDA and substrate. Figure 1 shows no sigmoid but does show a persistent linearity in the first two half-lives suggesting muted autocatalysis. We developed a method for detecting low levels of mixed aggregation effects using serial substrate injections as follows.

In a routine control experiment the IR baseline is zeroed at the end of a pseudo-first-order kinetic run, and a second aliquot of substrate is added. In the absence of autocatalysis, the rate for the second aliquot should show a minor decrease relative to the first aliquot because of the slight loss in LDA titer. In the 1,4-addition, however, the second aliquot afforded a measurably *higher* rate. This effect was amplified by serially injecting aliquots containing

10 mol % of ester **1** until the LDA was completely consumed. The initial rates are plotted versus mole fraction of enolate **5** (X_{ROLi}) in Figure 13. The serial injections correspond to movement from left to right along the *x*-axis.23 Figure 13 differs from a standard plot of concentration versus time in that (1) the normal upward curvature resulting from substrate loss has been factored out by adding substrate at constant concentrations and monitoring initial rates, and (2) all aggregates are allowed to equilibrate between injections.

$$-\Delta[\text{ester}_0]/\Delta t_0 = k[X_{ROLi}]^n[1 - X_{ROLi}]^m + k'[1 - X_{ROLi}]^{1.0} \quad (4)$$

The maximum at X_{ROLi} = 0.5 in Figure 13 suggests a 1:1 LDA/enolate ratio is optimal.23,24 The function in Figure 13 corresponds to a nonlinear least squares fit to eq 4 (see supporting information). This behavior could arise either from a key condensation involving LDA dimer **3** and enolate dimer **5a** (affording the mathematically equivalent 2:2 stoichiometry) or from mixed dimer **4** maximized at X_{ROLi} of 0.5. There is, however, a telling paradox: Figure 13 suggests that a 1,4-addition from equimolar mixtures of LDA and ester **1** should be markedly faster at 50% conversion than at the start. Nonetheless, there is no sigmoidal behavior in Figure 4—only a gentle straightening of the decay. (Perfect linearity arises if the autocatalysis precisely offsets the consumption of LDA.11)

Using ^{6}Li NMR spectroscopy we monitored the reaction of LDA dimer **3** and enolate dimer **5a** to give mixed dimer **4**. The reaction using 0.05 M each of **3** and **5a** revealed a half-life of 3000 seconds. First order dependencies in **3** and **5a** (Figures 14 and 15) in conjunction with a zeroth-order THF dependence (supporting information) afforded the idealized33 rate law in eq 5. The associative exchange suggests mixed-tetramer-based exchange.38 We can imagine ladder-based intermediates (eq 6),39,40 but monomeric LDA is not necessarily formed during the exchange, and the role this exchange plays in the 1,4-addition is minor at best (vide infra).41

$$-d[\mathbf{1}]/dt = k[A_2S_2][E_2][S]^0 \quad (5)$$

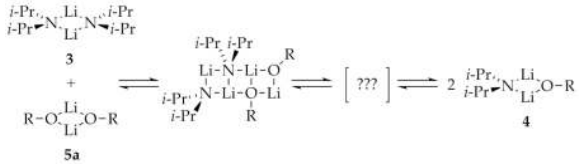

(6)

LiCl-Catalyzed 1,4-Additions

Very low concentrations of LiCl (<0.5 mol % relative to LDA) cause marked accelerations of the 1,4-addition and impart upward curvatures in plots of ester concentration versus time (Figure 1), which suggests that LiCl catalysis brings ester **1** into the rate law. The decays become cleanly first order at >0.5 mol % LiCl under pseudo-first-order conditions. Plotting the initial rates versus LiCl concentration reveals saturation kinetics with rates that plateau at >0.5 mol % LiCl (Figure 16).42

Saturation often arises when a bimolecular reaction at low concentration becomes unimolecular at higher concentrations because an observable complex is formed.43 Enzymology offers a plethora of examples under the rubric of Michaelis-Menten kinetics.44 A Michaelis-Menten-like saturation behavior, however, would require ≥100 mol % LiCl to

observably form LDA-LiCl mixed aggregates **6** and **7** as the dominant species, not a mere 0.5 mol %.45

Saturation kinetics can also be caused by a change in the rate-limiting step.43 Indeed, our rate studies are consistent with a scenario in which LiCl catalyzes a dimer-monomer exchange (eq 7). (Competition studies described below confirm this assertion.) The mechanism at full saturation (1.0 mol % LiCl) is gleaned from plots showing a half-order LDA dependence (Figure 17) and zeroth-order THF dependence (Figure 18). The equilibrium approximation affords the idealized33 rate law (eq 9), implicating a monosolvated-monomer-based transition structure ($[AS(ester)]^{\ddagger}$; eq 8).34 (ester = ester **1**, E = a subunit of enolate **5**, and $LiCl_T$ = lithium chloride titer). Importantly, although LiCl catalyzes the deaggregation, it has no role in the product-determining 1,4-addition step (eq 10).

$$\frac{1}{2}A_2S_2 \underset{k_{-1}[LiCl_T]}{\overset{k_1[LiCl_T]}{\rightleftharpoons}} AS \tag{7}$$

$$AS + ester \xrightarrow{k_2} [AS(ester)]^{\ddagger} \tag{8}$$

$$-d[ester]/dt = (k_1/k_{-1})^{1/2} k_2 [ester][S]^0 [A_2S_2]^{1/2} \tag{9}$$

We can now complete the mathematical analysis of the saturation curve in Figure 16. The transition from a rate-limiting deaggregation of dimer **3** in the absence of LiCl to a fully established pre-equilibrium at high $LiCl_T$ concentration precludes the equilibrium approximation. The concentrations of ester **1** and LDA dimer and monomer are described by eqs 10–12. Solving for the concentration of monomer AS in eq 10 using the quadratic equation and substituting into eq 8 affords the rate law in eq 13. (*c* corresponds to the low basal rate of uncatalyzed deaggregation.) The curve in Figure 16 corresponds to a fit to eq 13. Although eq 13 lacks the intuitive appeal of simple saturation functions, the rate reduces to *c* as $LiCl_T$ concentration approaches zero and to eq 9 at high $LiCl_T$ concentration.46

$$-d[ester]/dt = -k_2[ester][AS] \tag{10}$$

$$-d[A_2S_2]/dt = k_1[LiCl_T][A_2S_2] - k_{-1}[LiCl_T][AS]^2 \tag{11}$$

$$-d[AS_3]/dt = -2k_1[LiCl_T][A_2S_2] + 2k_{-1}[LiCl_T][AS]^2 + k_2[ester][AS] \approx 0 \tag{12}$$

$$-\frac{d[ester]}{dt} = \frac{k_2[ester]}{4k_{-1}[LiCl_T]}\left(\sqrt{k_2^2[ester]^2 + 16k_1k_{-1}[A_2]_0[LiCl_T]^2} - k_2[ester]\right) + c$$
$$(-d[ester]/dt = -\Delta[ester]/\Delta t_{(t=0)} \text{ by initial rates}) \tag{13}$$

Given the rate-limiting deaggregation in the absence of LiCl (eq 3), accelerating the deaggregation through LiCl catalysis logically accelerates the reaction. Why LiCl changes

the rate-limiting step is less obvious. Inspection of the mechanism in eqs 7 and 8 shows that elevated LiCl concentrations (k_{-1}[LiCl$_T$] >> k_2[ester]) cause the reaggregation to become competitive with the 1,4-addition, eventually affording a fully established pre-equilibrium. Thus, it is formally the catalysis of the *reaggregation* of LDA monomer by LiCl that causes the 1,4-addition to become rate limiting. Such reversibility is also required to observe a fractional-order dependence on LDA concentration.

The mechanism by which LiCl catalyzes the deaggregation of LDA is elusive, but a few comments are warranted. In LDA-LiCl mixtures containing low LiCl concentrations, LiCl exists exclusively as mixed aggregates **6** and **7** (1:8) to the exclusion of appreciable free LiCl.27,28 Thus, an apparent first-order dependence on the total LiCl concentration at the lowest LiCl concentration47 is tantamount to a first-order dependence on mixed aggregates. We repeat, however, that the mixed aggregates are relatively unreactive toward ester **1**.

With the monosolvated-monomer-based stoichiometry established for the addition at full LiCl catalysis, we turned to DFT computations. Transition structure **10** is plausible ($\Delta G^{\ddagger}$ = 16.3 kcal/mol at −78 °C, MP2 corrected), although the energy is large compared to the calculated barrier for the rate-limiting deaggregation (Scheme 1).

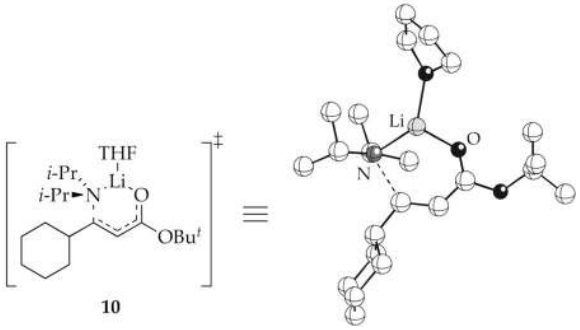

10

Competition Studies

We delineated three pathways for 1,4-addition that *may* share a common reactive intermediate: (1) uncatalyzed 1,4-addition with the key post-rate-limiting addition opaque to standard kinetic analysis; (2) autocatalyzed (enolate-mediated) deaggregation with the key 1,4-addition remaining post rate limiting; and (3) LiCl-catalyzed deaggregation with a rate-limiting 1,4-addition (eqs 7 and 8) shown to proceed via LDA monomer **11**. (We chose to draw the fleeting monomer **11** as the computationally most stable trisolvate.48) Standard protocols for examining post-rate-limiting steps to probe for common (shared) intermediates usually entail comparing inter- and intramolecular isotope effects.49 Showing that isotopic substitution affects the selectivity at a key branch point, but not the reaction rate, confirms the isotopically-sensitive step is post rate limiting. Given that the 1,4-addition is unsuited for isotopic labelling, we turned to a related approach using two structurally distinct substrates.

We established the reactivity of monomer **11** toward ester **1** and its *n*-alkyl analog **12**50 under conditions of fully saturated LiCl catalysis (eq 14). Whether in competition or in separate vessels, **12** displays a seven-fold greater reactivity. (We used gas chromatography to monitor mixtures of esters **1** and **12** for the competition experiments.) The 7:1 relative reactivity provides an important benchmark for monomer **11**.

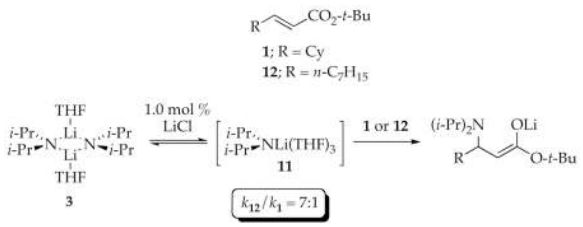

(14)

The uncatalyzed reaction of ester **1** with LDA involves a post-rate-limiting 1,4-addition: Is the key intermediate also monomer **11**? Ester **1** and *n*-alkyl analog **12** undergo 1,4-additions at indistinguishable rates despite differing steric demands, as expected for a rate-limiting deaggregation and post-rate-limiting 1,4-addition. By contrast, reacting an equimolar mixture of **1** and **12** with 2.0 equiv of LDA reveals a sevenfold greater reactivity of **12** relative to **1** (eq 15) as expected if monomer **11** is the intermediate. We also observe that once **12** is fully consumed, ester **1** reacts at a rate comparable to that of **12** (Figure 19). Such biphasic kinetics are expected for post-rate-limiting 1,4-additions.51

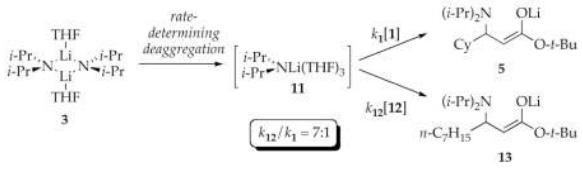

(15)

We suspected that the weak autocatalysis arose because ester enolate **5** is an inferior deaggregation catalyst compared to LiCl. A reaction was carried out to 50% conversion by adding 0.5 equiv of ester **1**—conditions to establish lithium enolate-induced acceleration—and subsequently treating the mixture with either **1** or **12** (separate reactions); the accelerations are indistinguishable for the two substrates. These results indicate that the formation of monomer **11** is still rate limiting, as expected for a catalyst that is poor compared to LiCl. By contrast, treating an analogous equimolar mixture of LDA and enolate **5** with an equimolar mixture of esters **1** and **12** shows a relative reactivity of 7:1. This confirms that the back reaction in eq 15—the reaggregation of LDA—is slow compared to the 1,4-addition (eq 16) and shows commonality of intermediates with both the uncatalyzed and the LiCl-catalyzed 1,4-additions.

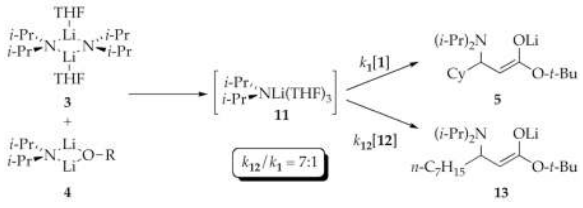

(16)

Mechanistic Hypothesis and Numeric Integrations.[52,53]

Rate and mechanistic studies were pieced together to form the mechanistic hypothesis shown in Scheme 2 and described by the affiliated differential equations in eqs 17–22. (Recall that A stands for an LDA subunit and E stands for an enolate subunit.) We have taken some liberties with the depiction of the model in Scheme 2 to optimize the visual presentation. Although the role of solvent has been elucidated for a number of steps, it is not germane to the numerical fits and has been omitted for clarity. We depict the critical autocatalytic step by affiliating k_3 and k_{-3} with fleeting mixed trimer A_2E; it is described numerically in the differential equations as an $A_2 + E \rightleftharpoons A + AE$ equilibrium. The equilibria in Scheme 2 are unbalanced to minimize clutter. The differential equations, by contrast, are all fully balanced to provide a valid mathematical description.

$$d[\text{ester}]/dt = k_2[\text{A}][\text{ester}] \tag{17}$$

$$d[\text{A}_2]/dt = -k_1[\text{A}_2] + k_{-1}[\text{A}]^2 - k_3[\text{A}_2][\text{E}] + k_{-3}[\text{A}][\text{AE}] \tag{18}$$

$$d[\text{A}]/dt = 2k_1[\text{A}_2] - 2k_{-1}[\text{A}]^2 - k_2[\text{A}][\text{ester}] + k_3[\text{A}_2][\text{E}] - k_{-3}[\text{A}][\text{AE}] - k_4[\text{A}][\text{E}] + k_{-4}[\text{AE}] \tag{19}$$

$$d[\text{AE}]/dt = k_3[\text{A}_2][\text{E}] - k_{-3}[\text{A}][\text{AE}] + k_4[\text{A}][\text{E}] - k_{-4}[\text{AE}] \tag{20}$$

$$d[\text{E}]/dt = k_2[\text{A}][\text{ester}] - k_3[\text{A}_2][\text{E}] + k_{-3}[\text{A}][\text{AE}] - k_4[\text{A}][\text{E}] + k_{-4}[\text{AE}] - 2k_5[\text{E}]^2 + 2k_{-5}[\text{E}_2] \tag{21}$$

$$d[\text{E}_2]/dt = k_5[\text{E}]^2 - k_{-5}[\text{E}_2] \tag{22}$$

It is nearly impossible to reproduce in prose how the model came into being, but we can describe the general strategy as well as the most critical constraints. We hasten to add at the outset that, despite aphorisms proclaiming that anything can be fit given enough differential equations, our experience with complex systems containing a large number of constraints and observables (see Figures 5–8) is quite the opposite. The model in Scheme 2 is the simplest model that fits the data, and many others fail to do so quite decisively.

First, a few comments about general tactics are warranted. The rate data place significant constraints on the model. In other instances seemingly reasonable hypotheses are excluded only through numerical simulations showing that key curvatures are not reproduced. Once the data in Figures 5–8 were qualitatively reproduced through numerical simulations, best-fit numerical integrations of eqs 17–22 afforded the functions displayed.

The key constraints imparted by the curvatures in Figures 5–8 include: (1) the linear decay of ester; (2) the two obvious discontinuities (most easily seen in Figure 8)—the maximum in enolate dimer (E_2) concentration and the marked change in rate of formation of the mixed dimer (AE) concentration—that coincide with the consumption of ester; (3) an overshoot in the concentration of E_2 relative to the equilibrium population; and (4) the coincident

formation of AE and E_2 at the outset of the reaction (most easily observed in Figure 5), indicating that AE is *not* a requisite precursor to E_2 (or vice versa).54

The model was assembled as follows:

1. The rate-limiting deaggregation of A_2 gives monomer A, which subsequently reacts in a post-rate-limiting step with ester to give enolate. This enolate will necessarily form as monomer (E). Thus, the $A_2 \rightarrow A \rightarrow E$ sequence representing the top half of Scheme 2 is fully established by traditional kinetic methods.
2. The fate of enolate monomer E is quite obviously a central issue. The self-condensation of E is the logical source of E_2. (The other logical source would be direct reaction of AE with ester.) The condensation of A and E is an obvious source of mixed dimer AE. A critical insight was that the bifurcation of E to form E_2 and AE allows for their concurrent formation (no induction period in either).
3. Two factors elicited the inclusion of the pathways involving the condensation of E with A_2 (via A_2E) to give mixed dimer AE and monomer A. (To reiterate, this is modeled as a net conversion and does not connote a single barrier pathway.) The most obvious is that the numerical simulations failed to reproduce the curvatures. *How* the simulations failed was key in that the simulations kept suggesting a source of AE independent of the simple reaggregation of A and E. Of course, there was considerable experimental evidence of autocatalysis, which can only arise by accelerating the rate-limiting deaggregation of LDA dimer A_2.
4. One might ask why the autocatalytic step is depicted as proceeding via A_2E rather than through a dimer-dimer condensation via A_2E_2. Again, the simple answer is that no amount of tinkering could force the curves to fit using an A_2E_2-based pathway. One can justify a provision for A_2E_2 *in addition to* A_2E based on the kinetics of mixed aggregation described in eqs 5 and 6, but the improvement in the fit is statistically insignificant.

The components of the model in Scheme 2 are well founded by the rate and mechanistic studies. As can be seen from Figures 5–8, the best-fit numerical integrations to eqs 17–22 are exceptional.

Discussion

It is becoming evident that reactions of LDA in THF at −78 °C are mechanistically complex even by the standards of organolithium chemistry.11,12 Nature could not have chosen a more inauspicious opportunity—a more synthetically relevant reagent under the most commonly used conditions—to insert confusion. The complexity stems from aggregate exchanges that occur at rates comparable to those of reaction with substrate.10 The result is that aggregation events can become rate limiting, and LDA-containing aggregates are not at full equilibrium on the time scales of their reactions with substrates. The first detailed investigations of such phenomena focused on ortholithiations of fluorinated aryl carbamates.11 Almost perfectly linear decays normally attributed to zeroth-order ester dependencies were traced to the superposition of a *first*-order ester dependence and autocatalysis. In the case of the 1,4-addition, seemingly analogous linear decays were traced to the superposition of a *zeroth*-order ester dependence and much less pronounced autocatalysis. A summary of the mechanism customized for mathematical treatment is provided in Scheme 2. The more structurally illuminating version with the full complement of intermediates and transition structures is summarized in Scheme 3. A compartmentalized summary follows.

Rate-Limiting Deaggregation

Monitoring the initial rates of the uncatalyzed 1,4-addition to ester **1** revealed a true zeroth-order dependence: deaggregation of LDA is rate limiting, and the 1,4-addition step is post rate limiting. The trisolvated-dimer-based deaggregation is either a partial deaggregation to form open dimer35 via transition structure **8** or a complete deaggregation to form monomer via transition structure **9**. Computational studies support **9** as the higher barrier. Even if the rate-limiting step involves formation of open dimer via **8**, however, standard rate studies do not peer past the rate-limiting step to distinguish a monomer-based from a dimer-based reaction with ester **1**. A combination of rate studies in the presence of LiCl and competition studies (both discussed below) support monomeric intermediate **11** and monosolvated-monomer-based transition structure **10**.

Autocatalysis

The rate-limiting deaggregation of dimer **3** that is dominant at the onset of 1,4-addition is overlayed by contributions from muted autocatalysis as the reaction progresses. It is very tempting to focus on mixed dimer **4** for explanation, but that would be wrong. Neither the elevated concentration nor higher reactivity of mixed dimer **4** causes autocatalysis. Mixed dimer **4** could react with ester **1** instantaneously, and it would *still* not constitute autocatalysis. An autocatalyst *must* catalyze the rate-limiting deaggregation of LDA. To understand autocatalysis it is instructive to focus on the structurally simplified model in Scheme 2.

Autocatalysis stems from accelerating the rate-limiting deaggregation of LDA dimer denoted as A_2. Notably, enolate homodimer E_2 is an ineffectual catalyst: enolate dimer reacts with LDA dimer *very* slowly. The autocatalysis was traced to the reaction of enolate *monomer* E. When LDA monomer A reacts with ester to form enolate monomer E, E can dimerize to form E_2 or react with an LDA monomer A to form mixed dimer AE. Occasionally, however, E reacts with LDA dimer A_2 to form AE and monomer A. *This* is autocatalysis.

The data, however, seem paradoxical. A plot of reaction rate using equimolar LDA and ester (Figure 4) shows some straightening that hints at autocatalysis, but a marked sigmoidal decay characteristic of virulent autocatalysis is notably absent. In short, the reaction is *not* faster at 50% conversion. By contrast, however, incremental additions of ester **1** to LDA illustrated in Figure 13 show a marked increase in rate with each increment, reaching a net fourfold higher rate at 50% consumption of LDA and 50% formation of enolate. An analogous fourfold autocatalysis certainly would have elicited quite distinct sigmoidal curvature in Figure 4.

How do we reconcile these two contrasting views? The key to understanding Figure 13 is to note that under normal reaction conditions the aggregates are *not* at full equilibrium, causing LDA-enolate mixed dimer AE to remain well below its equilibrium concentration. By contrast, the incremental additions in Figure 13 allow full aggregate equilibrations between increments. As a consequence, AE attains substantial equilibrium concentrations. When the subsequent increment of ester is added, the key LDA monomer is generated either from a rate-limiting deaggregation of A_2 or by a more facile (and only partially rate-limiting) deaggregation of mixed dimer AE. The rate maximum in Figure 13 corresponds to the maximum concentration of the kinetically labile AE mixed dimer. Thus, an experiment initially intended to explicitly probe autocatalysis uncovered an altogether different mixed aggregation effect. We will return to these distinctions below.

LiCl Catalysis

The 1,4-addition of LDA to ester **1** is measurably accelerated by as little as 0.001 mol % LiCl—*1.0 ppm*. At the risk of stating the obvious, we note that this is remarkably efficient catalysis.13 Readers might be unsurprised that this catalysis plagued the rate studies until we adapted protocols for preparing rigorously LiCl-free LDA from lithium metal.20 (Ironically, the modified synthesis is also more convenient than our standard method.)

Lithium chloride accelerates the 1,4-addition by catalyzing the deaggregation of LDA as summarized in eqs 7 and 8. Saturation behavior (Figure 16) with an onset of saturation at >0.5 mol % LiCl derives from a LiCl-catalyzed exchange of LDA dimers and monomers, resulting in a change from rate-limiting deaggregation to rate-limiting 1,4-addition. How LiCl catalyzes LDA deaggregation is still hazy and the subject of ongoing investigations. Nonetheless, rate studies revealed a monomer-based pathway for the addition, and computational studies filled in the intimate details in the form of transition structure **10**.

Competition Studies: Commonality of Intermediate

Competing esters **1** and **12** with different steric demands allowed us to probe post-rate-limiting reactivity (eqs 14–16). These studies are tactically analogous to comparisons of inter- and intramolecular isotope effects.50

The substrate-dependent rates under LiCl catalysis show that the 1,4-addition is rate limiting. Ester **12** is seven times more reactive than ester **1** toward monomer **11** (eq 14) both in separate reactions and in competition. Most important, this 7:1 preference serves as a benchmark for the monomer-based addition.

In the 1,4-addition under *uncatalyzed* conditions in which a partial or total deaggregation is rate limiting, the rates of 1,4-addition are identical for **1** and **12** when measured independently, which confirms a post-rate-limiting addition. Using mixtures of **1** and **12** in competition, however, produces the same sevenfold higher reactivity of **12** (eq 15) characteristic of trapping of monomer **11**.

A competition was carried out using equimolar mixtures of LDA and lithium enolate **5** to examine the influence of mixed dimer **4** (eq 16). When compared independently, esters **1** and **12** show identical reactivities, indicating that the deaggregations of **3** *and* **4** remain rate limiting. In contrast, a competition of **1** and **12** revealed the sevenfold greater reactivity of **12** characteristic of reaction with monomer **11**.

Do the 7:1 selectivities for the uncatalyzed, LiCl-catalyzed, and enolate-mediated additions *rigorously* show commonality of intermediate **11** and transition structure **10**? In a word, no. The selectivities do, however, make for a compelling circumstantial case.

Mixed Aggregation Effects: Four Variants

Effects of lithium salts on organolithium reactivity—so-called mixed aggregation effects—were first documented decades ago.14 Examples of mixed aggregation effects on rates and selectivities, whether LiX salts are added explicitly or formed in situ, are now legion.13 Mechanistically well-defined examples, however, are quite rare by comparison.15 We take this opportunity to discuss four distinct classes of mixed aggregation effects using LDA emblematically.

Case 1—Probably the most often cited and certainly the most intuitively simple salt effect derives from the direct reaction of mixed aggregates (such as **4**, **6**, and **7**) with substrates (eq 23). Because the steric and electronic properties of LDA-LiX mixed aggregates are

markedly different than those of homoaggregated LDA dimer **3**, and the LiX salt is assumed to be strategically located in the rate- and product-determining transition structures, it is easy to understand how LiX could markedly influence both rates and selectivities. We have documented direct reaction of LDA mixed dimers.15 Although the mixed aggregates could be either fleetingly stable or observable quantitatively, inhibition by observable mixed aggregates is prevalent.15,55 The critical requirement common to all examples in case 1, whether inhibiting or catalyzing, is that the LiX salt remains intimately involved in the rate- or product-determining transition structure.

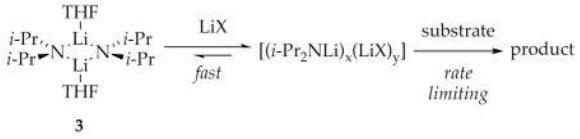

3

(23)

Case 2—Rate reductions are not the only consequence of inhibition. Imagine that a mixed aggregate forms quantitatively and shows no reactivity toward substrate (eq 24). The only available avenue of reaction is via free LDA. To the extent that the steady-state concentration of LDA is decreased to very low levels—a dilution of sorts—monomer-based pathways will be promoted relative to dimer-based pathways.56 The influence of such a mass action effect on the efficacy of monomer- and dimer-based pathways is illustrated in eq 25.15 Indeed, an LDA-dimer-based ester enolization was diverted by an intervening LDA-lithium enolate mixed dimer through both mixed dimer- *and* monomer-based pathways. To the extent that LiX can divert a dimer-based pathway to a monomer-based pathway, an LiX-dependent change in selectivity could arise *without intimate association of LiX with the product-determining transition structure*.

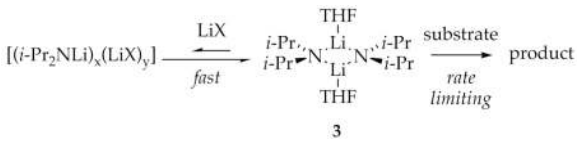

3

(24)

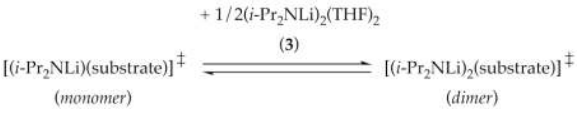

(25)

Case 3—The mixed aggregation effects described in this paper involve the LiX-catalyzed deaggregation. We must point out that there is jargon in the literature that loosely refers to LDA-LiX mixed aggregates as deaggregated because the mixed aggregate contains only one LDA subunit. We find this usage unconstructive. In the case described herein, however, the role of LiX salts—LiCl and, to a much lesser extent, lithium enolate—is to catalyze the formation of true LDA monomer (eq 26). To the best of our knowledge, this catalysis is undocumented. It will only be observed for reactions in which deaggregation is either rate limiting or is precluded altogether by a high barrier (forcing reaction out of the aggregated

form). No catalysis by LiCl will be observed if all aggregation states fully equilibrate on the time scales of reaction without added catalyst. Of course, to the extent that a rate-limiting deaggregation is accelerated, the overall reaction will be accelerated also. If that catalysis affords the same intermediate as the uncatalyzed deaggregation (monomer **11**), only faster, then the accelerations and even changes in the rate-limiting step will *not* be accompanied by changes in regio- or stereoselectivities. If, however, the preferred pathway for an uncatalyzed reaction is *dimer*-based because of a prohibitively high barrier to deaggregation, and LiX catalyzes monomer formation, the acceleration could be accompanied by a change in selectivity. We suspect that regioselective ortholithiations may be a fruitful place to look for such phenomena.

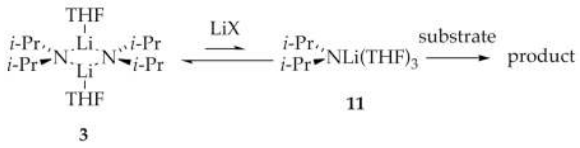

(26)

Case 4—In cases 1 and 2 we implicitly assume the aggregate exchanges are fast relative to reactions with substrate. Under this criterion, mixed aggregation will necessarily inhibit a reaction according to the principle of detailed balance56 unless the mixed aggregate can react with the substrate directly and rapidly. Case 4 addresses the consequences of mixed aggregation when aggregate exchanges are *not* at equilibrium during the course of the reaction. If, for example, deaggregations of LDA dimer **3** and mixed dimer **4** are rate limiting—if reaction with LDA monomer is at least competitive with reaggregation as the model in Scheme 2 suggests—the result would be a scenario in which facile deaggregation of mixed dimer **4** increases the rate that monomeric LDA is released and subsequently trapped. This is not formally autocatalysis because autocatalysis requires a provision for accelerating the deaggregation of LDA dimer **3**. Solutions containing considerable concentrations of labile mixed dimer **4**, however, would show a higher reactivity than that of analogous solutions with only LDA dimer **3**. This scenario accounts for 1,4-additions in the presence of enolate that are more rapid than would be predicted based on the low levels of autocatalysis.

Conclusion

A number of consequences of the work described herein are clear. Because traces of LiCl may contaminate LDA, source and batch dependencies could become acute. Synthetic chemists carrying out LDA-mediated reactions in THF at −78 °C might notice enormous differences between commercial LDA (which tends to be LiCl free) and LDA generated in situ from *n*-BuLi (which contains ample LiCl to catalyze exchanges). Indeed, this is the case for the 1,4-addition in eq 1. Adding traces of LiCl (in the form of Et_3NHCl) to commercial LDA equalizes the two protocols. Moreover, marked catalysis by traces of LiCl and inhibitions by molar excesses of LiCl suggest that the quantities of LiCl are important. We are reminded of LDA-mediated 3-pentanone enolizations in which the *E/Z* selectivities are maximized using fractional equivalents of LiCl.28 Could a composite of mixed aggregation effects be operative? We have long believed that deconvoluting the roles of LiCl in *E*-selective ketone enolizations would remain outside our grasp, but we are not so pessimistic now. We have also reported LiCl-accelerated ortholithiations in which traces of LiCl dramatically accelerated the rates but have *no* influence on regiocontrol because the regioisomers fully equilibrate.57 Some LDA-mediated ortholithiations are *not* at

equilibrium,58 however, and may display regioselectivities that *are* sensitive to traces of LiCl.

It is instructive to look forward. We have now reported two extensive studies of LDA-mediated reactions in which inordinate complexity rears its ugly head under conditions favored by synthetic chemists—LDA/THF/−78 °C. This is no bizarre coincidence: under these conditions aggregation events occur with half-lives on the order of minutes. *Any* LDA/THF-mediated reaction that proceeds on similar time scales at −78 °C will be subjected to potentially rate-limiting deaggregation and display a hypersensitivity to added lithium salts. Subtle changes in substrate reactivity and product structure (autocatalyst) could cause marked shifts in the relative efficacies of the competing steps and consequent baffling changes in rate behavior. Ongoing studies suggest that there may even be several rate-limiting LDA deaggregations (depending on choice of substrate) and several variants of autocatalysis. We are becoming increasingly certain that many—possibly all—LDA/THF-mediated reactions carried out at −78 °C are influenced by the rates at which aggregates exchange.

We close with a caveat, but not one readers may expect. In the earliest studies of organolithium chemistry, when the role of mixed aggregates was beginning to surface, salt effects were often couched in a mechanistic context and language that were inadequate. Chastened by that experience and the daunting mechanistic and structural complexity, specialists often warn non-specialists against invoking overly simplistic interpretations of salt effects on organolithium rates and selectivities. We admit some schadenfreude when uncovering complexity that undermines conventional mechanistic views, but it would be unfortunate if speculation —even unsubstantiated speculation—becomes stifled.

Experimental Section

Reagents and Solvents

THF and hexanes were distilled from blue or purple solutions containing sodium benzophenone ketyl. The hexanes contained 1% tetraglyme to dissolve the ketyl. Esters **1** and **12** were prepared via literature protocols.22,50 Et_3NHCl was recrystallized from THF/2-propanol.

Preparation and purification of LDA

Literature procedures20 were modified to prepare LDA as a LiCl-free and ligand-free solid as follows. A 250 ML Schlenk flask with attached fine-mesh glass frit and a 250 mL receiving flask was charged with lithium shavings (1.11 g, 160 mmol), diisopropylamine (16.5 g, 160 mmol), and 80 mL Me_2NEt. The flask was submerged in a bath at 25 °C and isoprene (5.44 g, 80 mmol) in 30 mL dry Me_2NEt added over 1.0 h via syringe pump. The solution was stirred for 1.0 h at 35 °C until the lithium dissolves. (The reaction exothermed if isoprene was added too quickly, affording highly undesirable dark yellow or purple solutions if the temperature exceeded 35 °C.) The nearly homogenous reaction was filtered through a fine-mesh glass frit and the solvent removed under vacuum (approximately 6 hr) to afford LDA as a white solid (16.0 g, 90% yield). With the aid of a glove box, the LDA (8.0 g) was transferred to a 250 mL round-bottomed flask fitted with a fine-mesh glass frit and a 250 mL pear-shaped receiving flask fitted with a side arm/stop-cock. The apparatus was attached to a vacuum line, and approximately 200 mL of hexanes was vacuum transferred into the flask containing the solid LDA. The solution was stirred at 63 °C (approximately 2 h) to afford a colorless solution of LDA; the flask was cooled to −78 °C by incrementally raising a dry ice/acetone bath to precipitate the LDA and held overnight at −78 °C. The mother liquor was carefully removed by filtration and the solid washed three times with 10 mL hexanes and then dried in vacuo for 6 h. The assembly was moved to the

glove box to collect the LDA as a white solid in 75–85% yield. The isolated material was spectroscopically indistinguishable from samples prepared previously.18

Synthesis of 2

Unsaturated ester **1** (0.63 g, 3.0 mmol) in 3.0 mL of THF was added to LDA (0.64 g, 6.0 mmol) in 15 mL of THF at −78 °C. The solution was stirred for 30 min and then warmed to room temperature with stirring for 1.0 h. The reaction was quenched with 10 mL of H_2O and extracted with diethyl ether (3 × 10 mL). The extracts were dried (Na_2SO_4), and the solvent was removed in vacuo. The residue was redissolved in CH_2Cl_2 (5 mL) and extracted with 4.0 M HCl (3 × 3 mL). The aqueous layer was neutralized with 10% NaOH and extracted with diethyl ether (3 × 5 mL). The combined organic layers were dried with $MgSO_4$, and the solvent was removed. Flash chromatography (30% ethyl acetate/hexane) afforded amino ester **2** (78–82% yield) with the spectral properties described previously.5

IR Spectroscopic Analyses

IR spectra were recorded using an in situ IR spectrometer fitted with a 30-bounce, silicon-tipped probe. The spectra were acquired in 16 scans at a gain of 1 and a resolution of 4 cm^{-1}, and the absorbance at 1715 cm^{-1} was monitored over the course of the reaction. For the most rapid reactions, IR spectra were recorded every 3 s.

A representative reaction was carried out as follows: The IR probe was inserted through a nylon adapter and O-ring seal into an oven-dried, cylindrical flask fitted with a magnetic stir bar and a T-joint. The T-joint was capped by a septum for injections and a nitrogen line. After evacuation under full vacuum, heating, and flushing with nitrogen, the flask was charged with LDA (107 mg, 1.00 mmol) in THF and cooled in a dry ice-acetone bath prepared from fresh acetone. LiCl (0.5 mol % relative to LDA) was added as a stock solution (0.50 mL) containing $Et_3N{\cdot}HCl$ (8.3 mg, 0.06 mmol) and LDA (13.5 mg, 0.12 mmol) in 5 mL THF. After recording a background spectrum, we added ester **1** (0.005 mmol) with stirring.

NMR Spectroscopic Analyses

All NMR tubes were prepared using stock solutions and sealed under partial vacuum. Standard ^6Li, ^{13}C, and ^{15}N NMR spectra were recorded on a 500 MHz spectrometer at 73.57, 125.79, and 50.66 MHz, respectively. The ^6Li, ^{13}C, and ^{15}N resonances are referenced to 0.30 M [^{6}Li]LiCl/MeOH at −90 °C (0.0 ppm), the CH_2O resonance of THF at −90 °C (67.57 ppm), and neat Me_2NEt at −90 °C (25.7 ppm), respectively.

Numeric Integrations

The time-dependent concentration plots obtained using ^6Li NMR spectroscopy (Figures 5–8) were fit to a mechanistic model expressed by a set of differential equations. The curve fitting minimized chi-square in searching for the coefficient values (rate constants). The Levenberg-Marquardt algorithm52 used for the chi-square minimization is a form of nonlinear, least-squares fitting. The fitting procedure implements numeric integration based on the backward differentiation formula53 to solve the differential equations, yielding functions describing concentration versus time.

Supplementary Material

Refer to Web version on PubMed Central for supplementary material.

Acknowledgments

We thank the National Institutes of Health (GM39764 and, in part, GM 077167) for direct support of this work and Pfizer, Merck, and Sanofi-Aventis for indirect support.

References and Footnotes

1. (a) Herrman JL, Kieczykowski GR, Schlessinger RH. Tetrahedron Lett. 1973:2433. (b) Doi H, Sakai T, Iguchi M, Yamada K, Tomioka K. J. Am. Chem. Soc. 2003; 125:2886. [PubMed: 12617650] (c) Uyehara T, Asao N, Yamamoto Y. J. Chem. Soc., Chem. Commun. 1987:1410. (d) Amputch MA, Matamoros R, Little RD. Tetrahedron. 1994; 50:5591. (e) Hase TA, Kukkola P. Synth. Commun. 1980; 10:451. (f) Inokuchi T, Kawafuchi H. J. Org. Chem. 2007; 72:1472. [PubMed: 17253744]
2. (a) Uyehara T, Asao N, Yamamoto Y. J. Chem. Soc., Chem. Commun. 1987:1410. (b) Bellasoued M, Ennigrou R, Gaudemar M. J. Organomet. Chem. 1988; 338:149.
3. Davies SG, Smith AD, Price PD. Tetrahedron: Asymmetry. 2005; 16:2833.
4. (a) Bakker, WII.; Wong, PL.; Snieckus, V. Lithium Diisopropylamide. In: Paquette, LA., editor. e-EROS. New York: John Wiley; 2001. (b) Clayden, J. “Organolithiums: Selectivity for Synthesis”. Baldwin, JE.; Williams, RM., editors. New York: Pergamon; 2002.
5. Ma Y, Collum DB. J. Am. Chem. Soc. 2007; 129:14818. [PubMed: 17985891]
6. For a review summarizing rate studies of LDA-mediated reactions: Collum DB, McNeil AJ, Ramirez A. Angew. Chem., Int. Ed. 2007; 46:3002.
7. For an attempted comprehensive bibliography of triple ions of lithium salts, see: Ma Y, Ramirez A, Singh KJ, Keresztes I, Collum DB. J. Am. Chem. Soc. 2006; 128:15399. [PubMed: 17132006]
8. (a) Espenson, JH. Chemical Kinetics and Reaction Mechanisms. 2nd ed.. New York: McGraw-Hill; 1995. p. 44Chapter 2Atkins, PW.; Jones, LL. Chemical Principles: the Quest for Insight. 2nd ed.. New York: W H. Freeman; 2002.
9. For other examples of odd linearities that may or may not have origins similar to those described herein, see: (a) Blackmond DG, Ropic M, Stefinovic M. Org. Proc. Res. Develop. 2006; 10:457. (b) Akao A, Nonoyama N, Mase T, Yasuda N. Org. Proc. Res. Develop. 2006; 10:1178. (c) Rowley JM, Lobkovsky EB, Coates GW. J. Am. Chem. Soc. 2007; 129:4948. [PubMed: 17397149] (d) Yin C-X, Finke RG. J. Am. Chem. Soc. 2005; 127:13988. [PubMed: 16201821]
10. For examples of reactions that are fast relative to the rates of aggregate-aggregate exchanges see: (a) McGarrity JF, Ogle CA. J. Am. Chem. Soc. 1985; 107:1810. (b) Jones AC, Sanders AW, Bevan MJ, Reich HJ. J. Am. Chem. Soc. 2007; 129:3492. [PubMed: 17341084] (c) Thompson A, Corley EG, Huntington MF, Grabowski EJJ, Remenar JF, Collum DB. J. Am. Chem. Soc. 1998; 120:2028. (d) Jones AC, Sanders AW, Sikorski WH, Jansen KL, Reich HJ. J. Am. Chem. Soc. 2008; 130(19):6060. [PubMed: 18419118] (e) See ref 11.
11. Singh KJ, Hoepker AC, Collum DB. J. Am. Chem. Soc. 2008; 130:18008. [PubMed: 19053473]
12. Gupta L, Hoepker AC, Singh KJ, Collum DB. J. Org. Chem. 2009; 74:2231. [PubMed: 19191711]
13. For leading references and discussions of mixed aggregation effects, see: (a) Seebach D. Angew. Chem., Int. Ed. Engl. 1988; 27:1624. (b) Tchoubar, B.; Loupy, A. Salt Effects in Organic and Organometallic Chemistry. New York: VCH; 1992. Chapters 4, 5, and 7. (c) Briggs TF, Winemiller MD, Xiang B, Collum DB. J. Org. Chem. 2001; 66:6291. [PubMed: 11559177] (d) Caubère P. Chem. Rev. 1993; 93:2317.
14. Seebach, D. Proceedings of the Robert A. Welch Foundation Conferences on Chemistry and Biochemistry; New York: Wiley; 1984. p. 93
15. Ramirez A, Sun X, Collum DB. J. Am. Chem. Soc. 2006; 128 10326 and references cited therein.
16. Evans, A. Potentiometry and Ion-Selective Electrodes. New York: Wiley; 1987.
17. Fuji T. Anal. Chem. 1992; 64:775.
18. Kim Y-J, Bernstein MP, Galiano-Roth AS, Romesberg FE, Fuller DJ, Harrison AT, Collum DB, Williard PG. J. Org. Chem. 1991; 56:4435.
19. Kottke T, Stalke D. Angew. Chem., Int. Ed. Engl. 1993; 32:580.Rennels RA, Maliakal AJ, Collum DB. J. Am. Chem. Soc. 1998; 120:421.

20. (a) Marck W, Huisgen R. Chem. Ber. 1960; 93:608. (b) Gaudemar-Bardone F, Gaudemar M. Synthesis. 1979:463. (c) Reetz MT, Maier WF. Liebigs Ann. Chem. 1980:1471. (d) Williard PG, Carpenter GB. J. Am. Chem. Soc. 1986; 108:462.Williard PG, Salvino JM. J. Org. Chem. 1993; 58:1. (e) Morrison, RC.; Hall, RW.; Rathman, TL., inventors. Stable Lithium Diisopropylamide and Method of Preparation. U.S. Patent. 4,595,779. 1986 June 17.
21. See Zhao P, Collum DB. J. Am. Chem. Soc. 2003; 125 14411 and references cited therein.
22. Lucht BL, Collum DB. J. Am. Chem. Soc. 1996; 118:3529.Waldmüller D, Kotsatos BJ, Nichols MA, Williard PG. J. Am. Chem. Soc. 1997; 119:5479.Sato D, Kawasaki H, Shimada I, Arata Y, Okamura K, Date T, Koga K. J. Am. Chem. Soc. 1992; 114:761.Reich HJ, Goldenberg WS, Gudmundsson BO, Sanders AW, Kulicke KJ, Simon K, Guzei IA. J. Am. Chem. Soc. 2001; 123:8067. [PubMed: 11506563] Johansson A, Davidsson O. 2001; 7:3461.Aubrecht KB, Lucht BL, Collum DB. Organometallics. 1999; 18:2981.
23. Job P. Ann. Chim. 1928; 9:113. For more recent examples and leading references, see: Huang CY. Method Enzymol. 1982; 87:509. Hubbard RD, Horner SR, Miller BL. J. Am. Chem. Soc. 2001; 123:5810. [PubMed: 11403619] Potluri V, Maitra U. J. Org. Chem. 2000; 65:7764. [PubMed: 11073578]
24. (a) Liou LR, McNeil AJ, Ramirez A, Toombes GES, Gruver JM, Collum DB. J. Am. Chem. Soc. 2008; 130:4859. [PubMed: 18336025] (b) Gruver JM, Liou LR, McNeil AJ, Ramirez A, Collum DB. J. Org. Chem. 2008; 73:7743. [PubMed: 18781812]
25. Frisch, MJ., et al. *Gaussian 03*; revision B.04. Wallingford, CT: Gaussian, Inc.; 2004.
26. (a) Reich HJ, Borst JP, Dykstra RR, Green DP. J. Am. Chem. Soc. 1993; 115:8728. (b) Wong MK, Popov AI. J. Inorg. Nucl. Chem. 1972; 34:3615. (c) Yakimansky AV, Müller AH, Beylen MV. Macromolecules. 2000; 33:5686. (d) Goralski P, Chabanel M. Inorg. Chem. 1987; 26 2169 and references cited therein.
27. Studies of LDA-LiCl at ultralow LiCl as well as confirmation of LiCl in THF as a dimer will be reported in due course.
28. Galiano-Roth AS, Kim Y-J, Gilchrist JH, Harrison AT, Fuller DJ, Collum DB. J. Am. Chem. Soc. 1991; 113:5053. Also, see: Hall PL, Gilchrist JH, Collum DB. J. Am. Chem. Soc. 1991; 113:9571.
29. Snaith and coworkers underscored the merits of R_3NHX salts as precursors to anhydrous LiX salts: Barr D, Snaith R, Wright DS, Mulvey RE, Wade K. J. Am. Chem. Soc. 1987; 109:7891. Also, see: Hall PL, Gilchrist JH, Collum DB. J. Am. Chem. Soc. 1991; 113:9571.
30. Rein AJ, Donahue SM, Pavlosky MA. Curr. Opin. Drug Discov. Develop. 2000; 3:734.
31. Addition of excess *i*-Pr_2NH to the metalation has no measurable effect on the rates or curvatures.
32. The concentration of LDA, although expressed in units of molarity, refers to the concentration of the monomer unit (normality).
33. We define the idealized rate law as that obtained by rounding the observed reaction orders to the nearest rational order.
34. The rate law provides the stoichiometry of the transition structure relative to that of the reactants: Edwards JO, Greene EF, Ross J. J. Chem. Educ. 1968; 45:381.
35. Open dimers were first proposed for the isomerization of oxiranes to allylic alcohols by mixed metal bases: Mordini A, Rayana EB, Margot C, Schlosser M. Tetrahedron. 1990; 46:2401. For a bibliography of lithium amide open dimers, see ref 15.
36. (a) Besson C, Finney EE, Finke RG. J. Am. Chem. Soc. 2005; 127:8179. [PubMed: 15926847] (b) Besson C, Finney EE, Finke RG. Chem. Mater. 2005; 17:4925. (c) Huang KT, Keszler A, Patel N, Patel RP, Gladwin MT, Kim-Shapiro DB, Hogg N. J. Biol. Chem. 2005; 280:31126. [PubMed: 15837788] (d) Huang Z, Shiva S, Kim-Shapiro DB, Patel RP, Ringwood LA, Irby CE, Huang KT, Ho C, Hogg N, Schechter AN, Gladwin MT. J. Clin. Invest. 2005; 115:2099. [PubMed: 16041407] (e) Tanj S, Ohno A, Sato I, Soai K. Org. Lett. 2001; 3:287. [PubMed: 11430056] (f) Barrios-Kabderism F, Carrow BP, Hartwig. J. Am. Chem. Soc. 2008; 130:5842. [PubMed: 18402444]
37. (a) Depue JS, Collum DB. J. Am. Chem. Soc. 1988; 110:5524. (b) McNeil AJ, Toombes GES, Gruner SM, Lobkovsky E, Collum DB, Chandramouli SV, Vanasse BJ, Ayers TA. J. Am. Chem. Soc. 2004; 126:16559. [PubMed: 15600361] (c) Nudelman NS, Velurtas S, Grela MA. J. Phys. Org. Chem. 2003; 16:669. (d) Alberts AH, Wynberg H. J. Am. Chem. Soc. 1989; 111:7265. (e) Alberts AH, Wynberg H. J. Chem. Soc., Chem. Commun. 1990:453.

38. Tetramer-based intermediates have also been implicated in LDA-mediated ortholithiations. Ma Y, Hoepker AC, Gupta L, Collum DB. unpublished.
39. A four-rung LDA/enolate ladder structure has been characterized crystallographically: Williard PG, Hintze MJ. J. Am. Chem. Soc. 1987; 109:5539.
40. (a) Gregory K, Schleyer PvR, Snaith R. Adv. Inorg. Chem. 1991; 37:47. (b) Mulvey RE. Chem. Soc. Rev. 1991; 20:167.(c) Beswick, MA.; Wright, DS. Comprehensive Organometallic Chemistry II. Abels, EW.; Stone, FGA.; Wilkinson, G., editors. Vol. Vol. 1. New York: Pergamon; 1995. Chapter 1 (d) Mulvey RE. Chem. Soc. Rev. 1998; 27:339. (e) Rutherford JL, Collum DB. J. Am. Chem. Soc. 1999; 121:10198.
41. (a) Paté F, Gérard H, Oulyadi H, de la Lande A, Harrison-Marchand A, Parisel O, Maddaluno J. J. Chem. Soc., Chem. Commun. 2009:319. (b) Arvidsson PI, Ahlberg P, Hilmersson G. Chem. Eur. J. 1999; 5:1348.
42. Saturation is also apparent by plotting the observed rate constants from fits to the exponential decays.
43. Espenson, JH. Chemical Kinetics and Reaction Mechanisms. 2nd ed.. New York: McGraw-Hill; 1995.
44. Frey, PA.; Hegeman, AD. "Enzymatic Reaction Mechanisms. New York: Oxford University Press; 2007. Chapter 2
45. In fact, addition of 100 mol % causes an three-fold *inhibition* compared to native LDA containing 1.0 mol % LiCl. Davies noted a similar inhibition of LiCl on the 1,4-additions of chiral lithium amides to unsaturated esters. LiCl had no measurable effect on the stereoselectivity. Davies SG, Hermann GJ, Sweet MJ, Smith AD. J. Chem. Soc., Chem. Commun. 2004:1128.
46. Equation 13 would appear to become undefined at $[LiCl_T] = 0$. This is not the case. Qualitatively, the $[LiCl_T]^2$ within the argument of the square root approaches zero at low values of $[LiCl_T]$ faster than the $[LiCl_T]$ in the denominator. Alternatively, let $a=k_2[\text{ester}]$, $b=16k_1k_{-1}[A_2]_0$, $d=4k_{-1}$ and $x=[LiCl_T]^2$. Eq 13 is rewritten as

$$\frac{-d[\text{ester}]}{dt} = \frac{a}{dx^{0.5}}[(a^2+bx)^{0.5} - a] + c = \frac{a}{dx^{0.5}}[a(1+\frac{b}{a^2}x)^{0.5} - a] + c$$

Applying the Taylor expansion to $(1+\frac{b}{a^2}x)^{0.5}$ for $x<<1$, gives

$$\frac{-d[\text{ester}]}{dt} = \frac{a}{dx^{0.5}}[a(1+\frac{b}{2a^2}x)^{0.5} - a] + c = \frac{bx}{2dx^{0.5}} + c$$

$$\lim_{x\to 0} \frac{bx}{2dx^{0.5}} + c = c$$

as x approaches zero faster than $x^{0.5}$.

47. Although the saturation behavior is not sigmoidal, excluding a higher-order dependency on LiCl, the data do not exclude a fractional LiCl dependence.
48. Viciu M, Gupta L, Collum DB. J. Am. Chem. Soc. 2010; 132:6361. [PubMed: 20397635]
49. (a) Carpenter, BK. Determination of Organic Reaction Mechanisms. New York: Wiley; 1984. (b) Whisler MC, MacNeil S, Snieckus V, Beak P. Angew. Chem., Int. Ed. 2004; 43:2206.
50. Davies SG, Mulvaney AW, Russell AJ, Smith AD. Tetrahedron: Asymm. 2007; 18:1554.
51. The curves in Figure 16 correspond to numerical integration to the highly simplified model as follows:

$$\tfrac{1}{2}\ A_2 \rightleftharpoons A$$

$$A + \mathbf{1} \rightarrow \mathbf{5}$$

$$A + \mathbf{12} \rightarrow \mathbf{13}$$

52. For an explanation of the Levenberg-Marquardt nonlinear least-squares optimization, see: Press, WH.; Flannery, BP.; Teukolsky, SA.; Vetterling, VT. Numerical Recipes in C. London: Cambridge University Press; 1988. Chapter 14.4
53. Brown PN, Byrne GD, Hindmarsh AC. J. Sci. Stat. Comput. 1989; 10:1038.

54. Given a reaction coordinate $SM \rightarrow I \rightarrow P$ in which I builds to appreciable concentrations, the rate of formation of P will show an induction period (ref 43).

55. (a) Sun X, Collum DB. J. Am. Chem. Soc. 2000; 122:2459. (b) See references in ref 6.

56. (a) The Principle of Detailed Balance asserts that individual equilibria within an ensemble of equilibria are maintained.57b,c,d It is particularly useful in understanding the complex equilibria observed in organolithium chemistry. (b) Alberty RA. J. Chem. Educ. 2004; 81:1206–1209. (c) Casado J, Lopez-Quintela MA, Lorenzo-Barral FM. J. Chem. Educ. 1986; 63:450. (d) Hammes, GG. Principles of Chemical Kinetics. New York: Academic Press; 1978. p. 14-15.

57. (a) Cottet F, Schlosser M. Eur. J. Org. Chem. 2004:3793. (b) Trecourt F, Mallet M, Marsais F, Quéguiner G. J. Org. Chem. 1988; 53:1367. (c) Comins DL, LaMunyon DH. Tetrahedron Lett. 1988; 29:773. (d) Eaton PE, Cunkle GT, Marchioro G, Martin RM. J. Am. Chem. Soc. 1987; 109:948. (e) Bridges AJ, Patt WC, Stickney TM. J. Org. Chem. 1990; 55:773. (f) Trécourt F, Marsais F, Güngör T, Quéguiner G. J. Chem. Soc., Perkin Trans. 1. 1990:2409. (g) Gros PC, Fort Y. Eur. J. Org. Chem. 2009:4199. (h) Cottet F, Marull M, Lefebvre O, Schlosser M. Eur. J. Org. Chem. 2003:1559. (i) Güngör T, Marsais F, Queguiner G. J. Organomet. Chem. 1981; 215:139.

58. (a) Schlosser M. Angew. Chem. Int. Ed. 2005; 44:376. (b) Schlosser M, Rausis T. Eur. J. Org. Chem. 2004:1018.

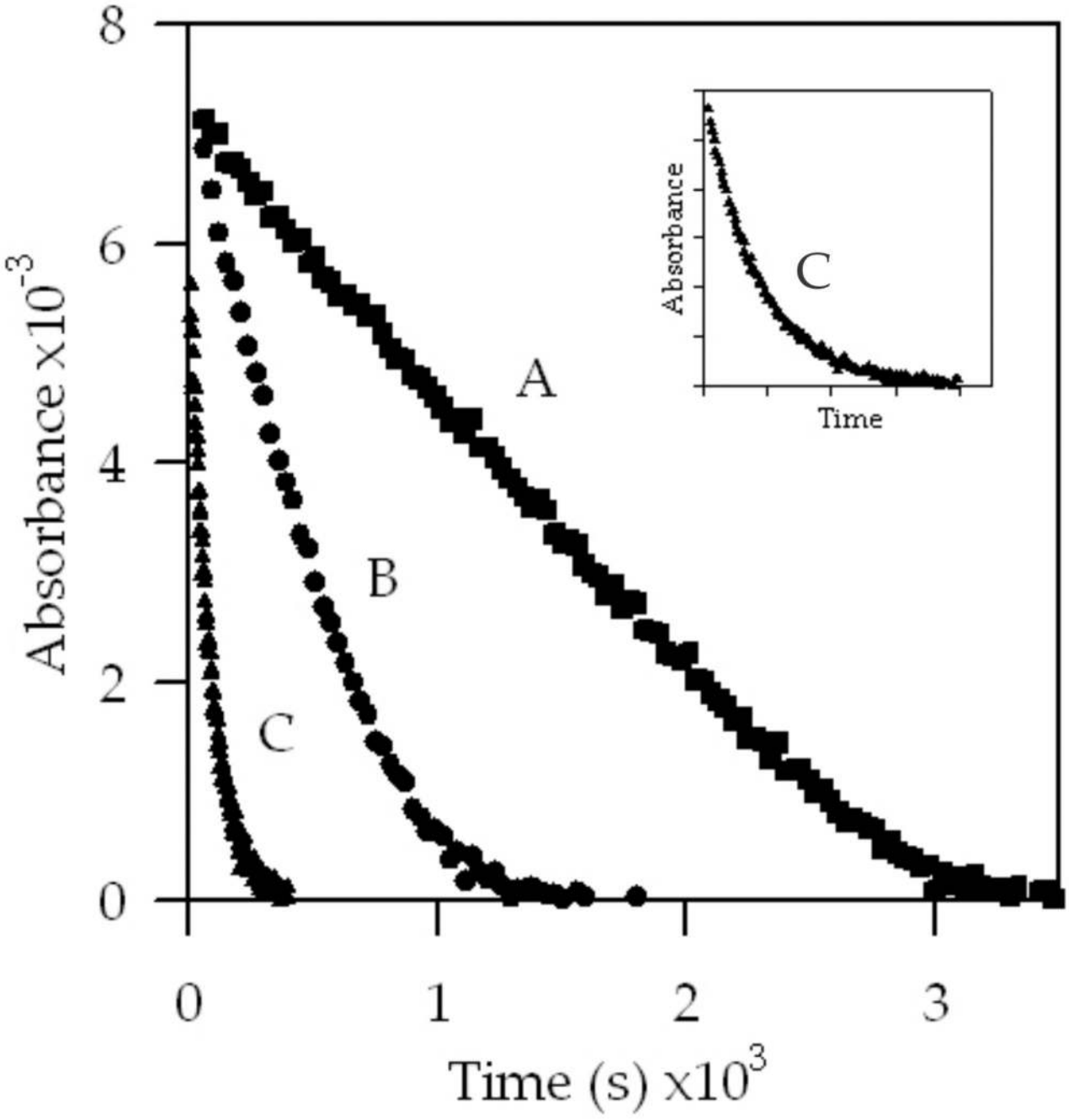

Figure 1.
Plot of IR absorbance vs time in THF (6.10 M) for 1,4-addition of ester **1** (0.004 M) with LDA (0.10 M) at −78 °C in the presence of varying mol % of LiCl: (A) no LiCl; (B) 0.01 mol % LiCl; (C) 0.4 mol % LiCl. The insert shows an expanded view of curve C.

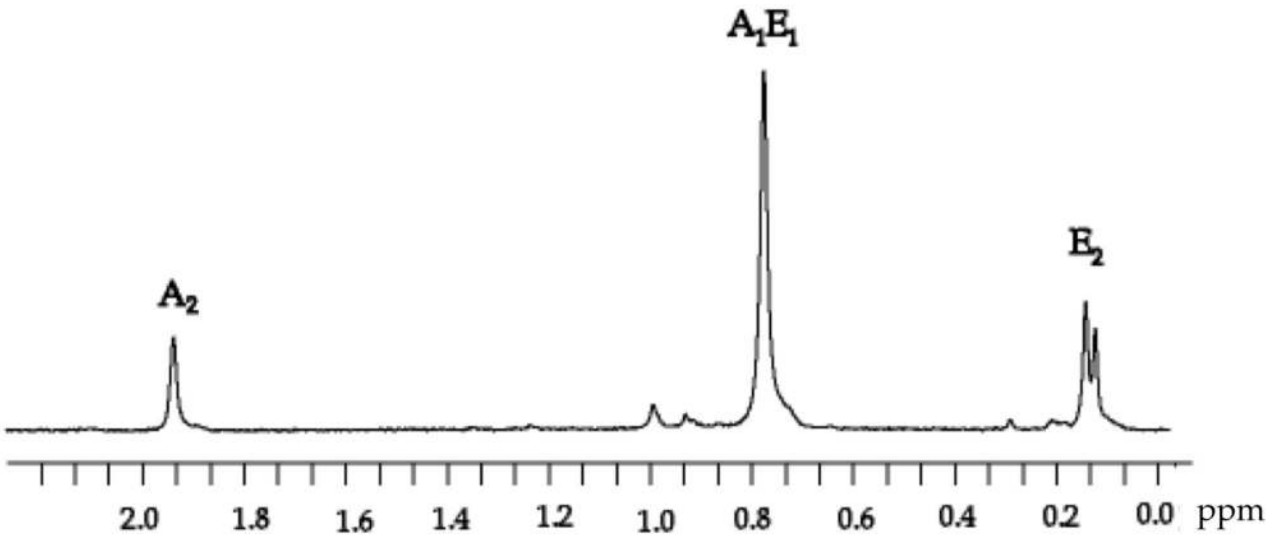

Figure 2.
Representative ^{6}Li NMR spectrum of a 60:40 mixture of [^{6}Li]**5** and[^{6}Li]**3** showing homodimers (A_2 and E_2) and mixed dimer [^{6}Li]**4** (AE).

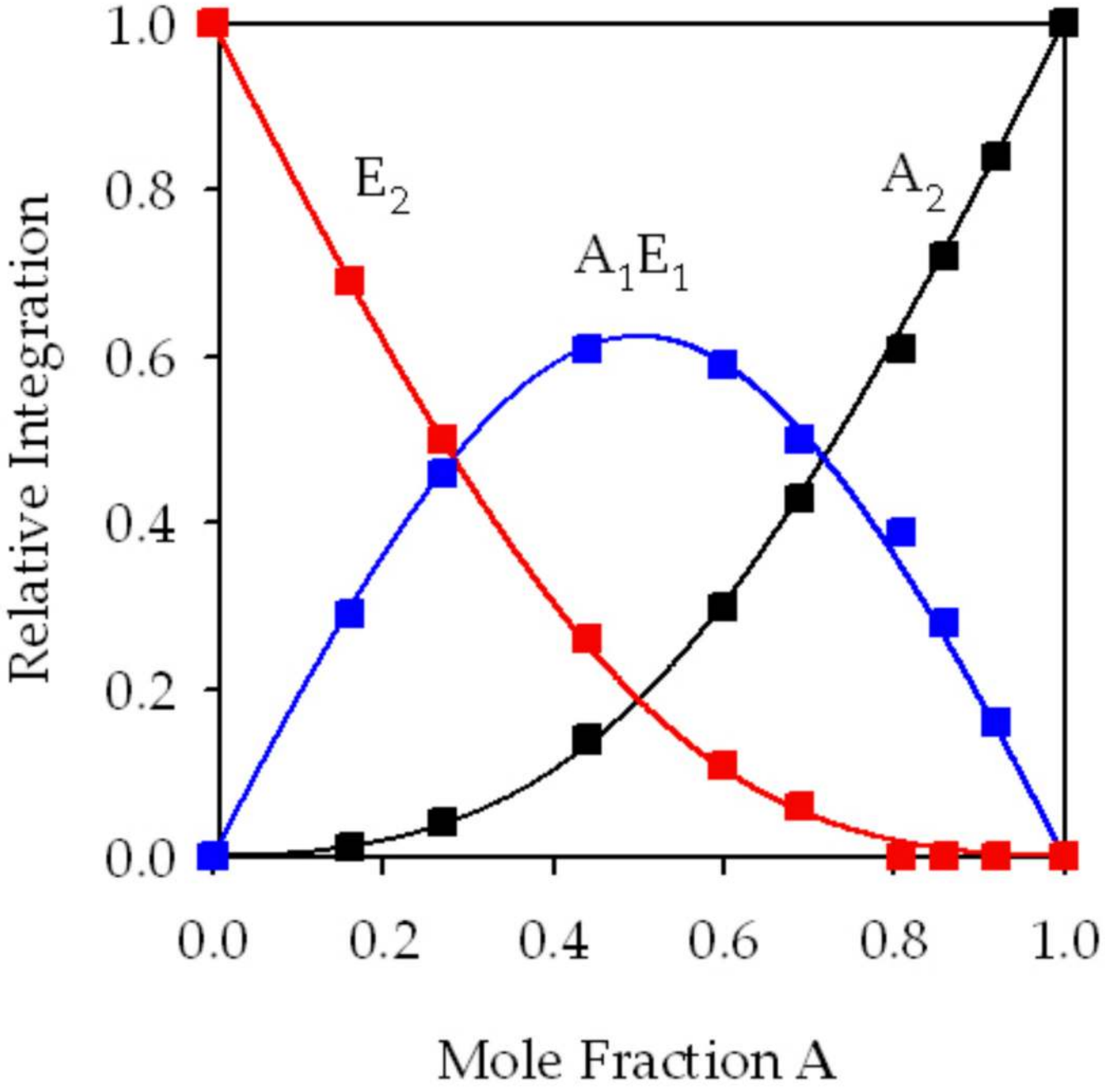

Figure 3.
Plot of the relative integration vs the mole fraction of [^{6}Li]**3**, [^{6}Li]**4**, and [^{6}Li]**5**. The curves derive from a parametric fit as described previously.24

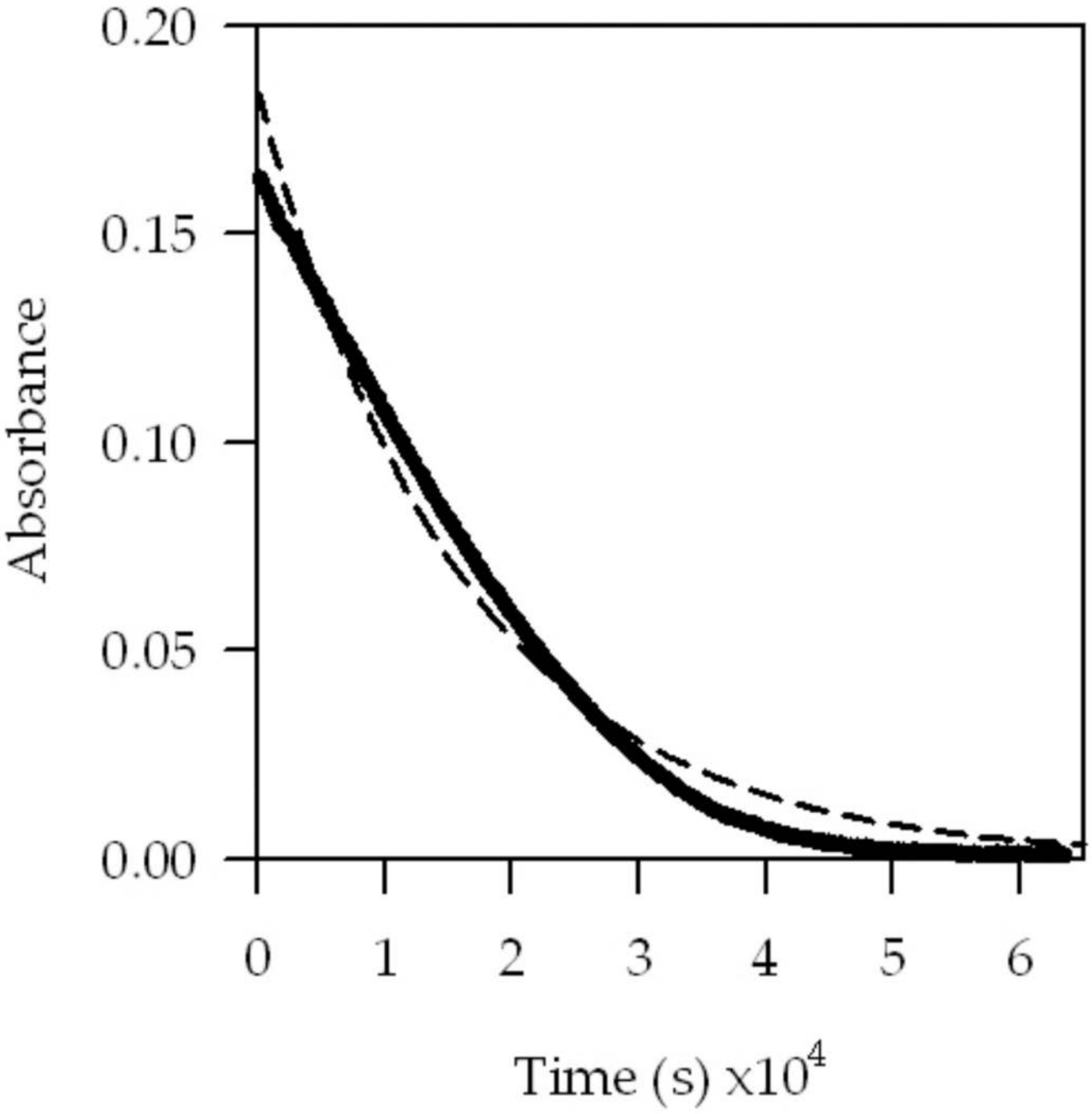

Figure 4.
Plot showing IR absorbance of ester **1** vs time for the 1,4-addition of ester **1** (0.10 M) with LDA (0.10 M) in neat THF at −78 °C. The dashed line shows the poor first-order fit ($y = ae^{bx}$).

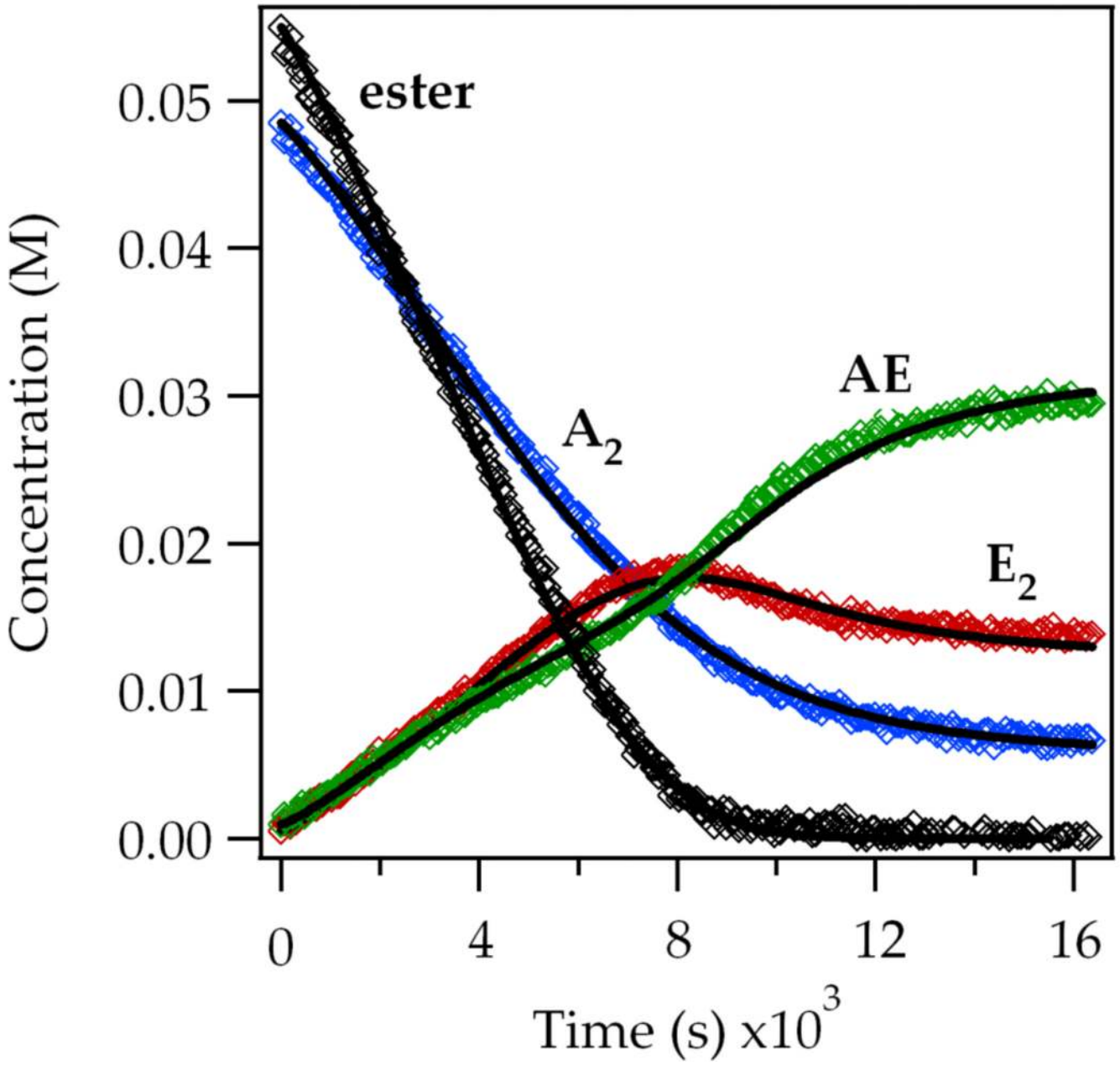

Figure 5.

Time-dependent concentrations measured by ^{6}Li NMR spectroscopy using 0.05 M **3** (0.10 *normal*), 0.05 M **1** in 6.1 M THF at −78 °C. Ester = **1**; A_2 = LDA dimer **3**; E_2 = enolate dimer **5a**; AE = enolate mixed dimer **4**. The curves represent a parametric fit to eqs 17–22 (described below). The best-fit values for the rate constants are listed in supporting information.

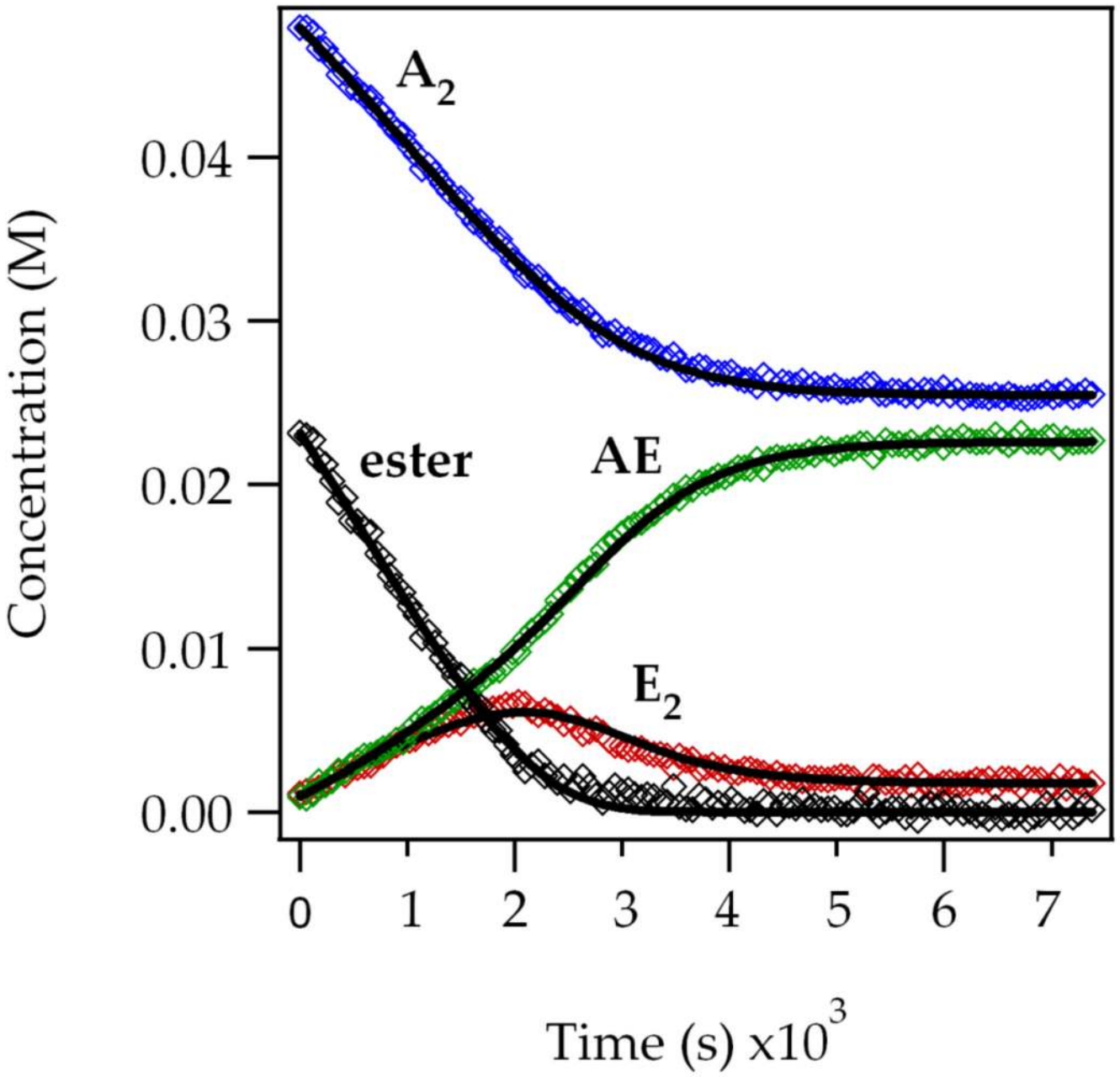

Figure 6.

Time-dependent concentrations measured by ^{6}Li NMR spectroscopy using 0.05 M **3** (0.10 *normal*), 0.025 M **1** in 6.1 M THF at −78 °C. Ester = **1**; A_2 = LDA dimer **3**; E_2 = enolate dimer **5a**; AE = enolate mixed dimer **4**. The curves represent a parametric fit to eqs 17–22 (described below). The best-fit values for the rate constants are listed in supporting information.

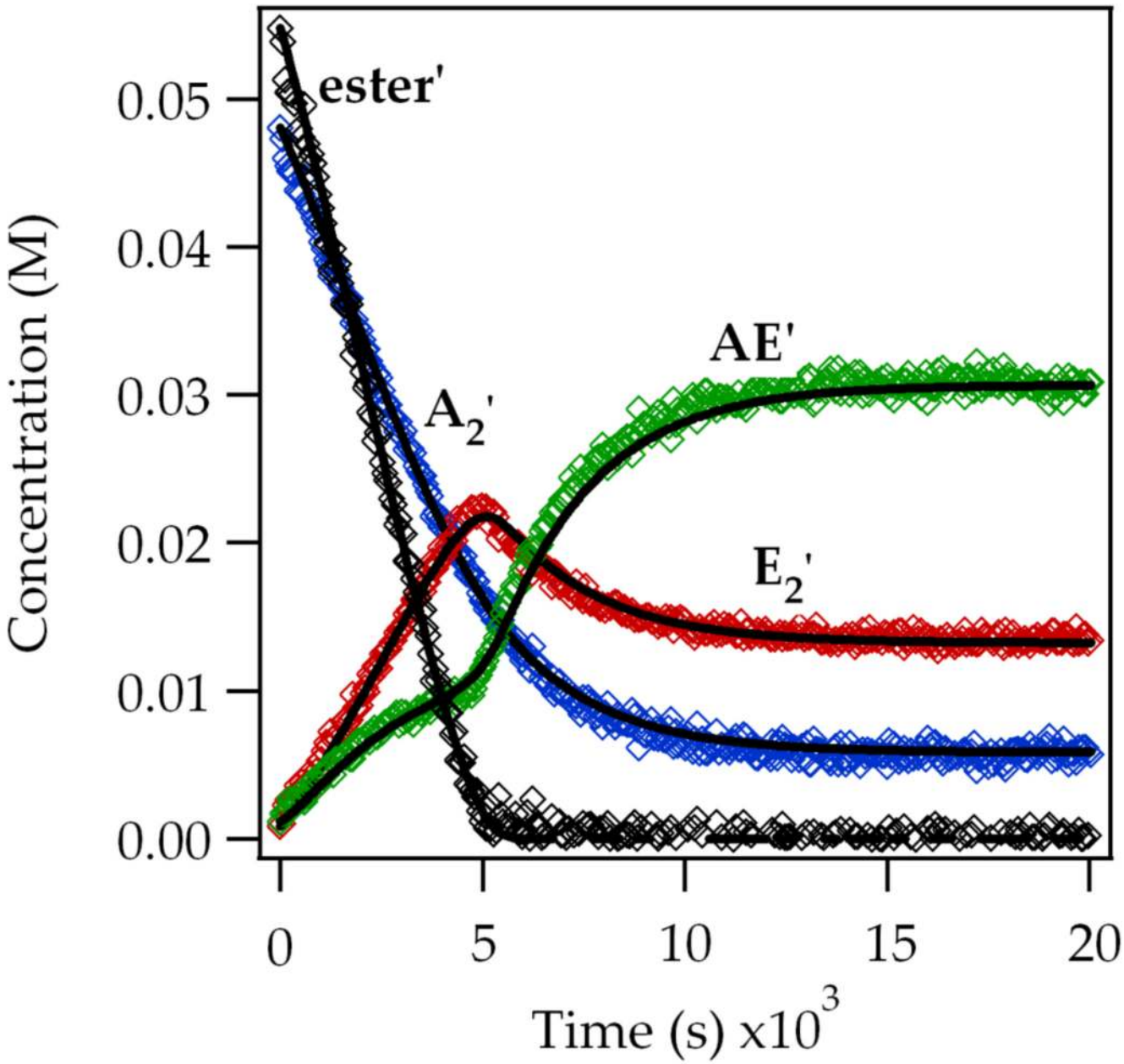

Figure 7.

Time-dependent concentrations measured by ^{6}Li NMR spectroscopy using 0.05 M **3** (0.10 *normal*), 0.05 M ester **12** in 6.1 M THF at −78 °C. Ester = **12**; A_2 = LDA dimer **3**; E_2 = enolate dimer of ester **12**; AE = enolate mixed dimer. The curves represent a parametric fit to eqs 17–22 (described below). The best-fit values for the rate constants are listed in supporting information.

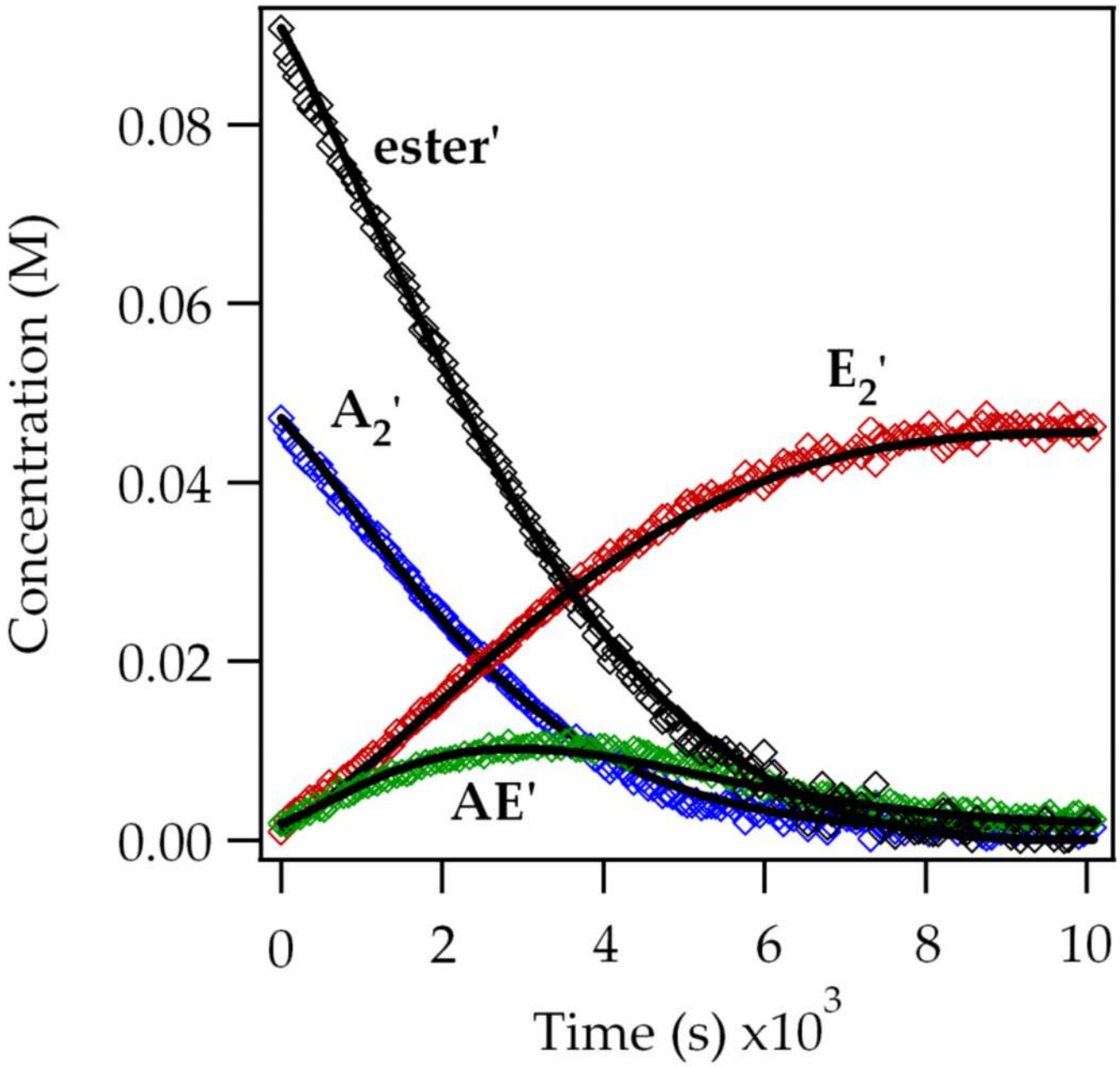

Figure 8.

Time-dependent concentrations measured by ^{6}Li NMR spectroscopy using 0.05 M **3** (0.10 *normal*), 0.10 M **12** in 6.1 M THF at −78 °C. Ester = **12**; A_2 = LDA dimer **3**; E_2 = enolate dimer of **12**; AE = enolate mixed dimer. The curves represent a parametric fit to eqs 17–22 (described below). The best-fit values for the rate constants are listed in supporting information.

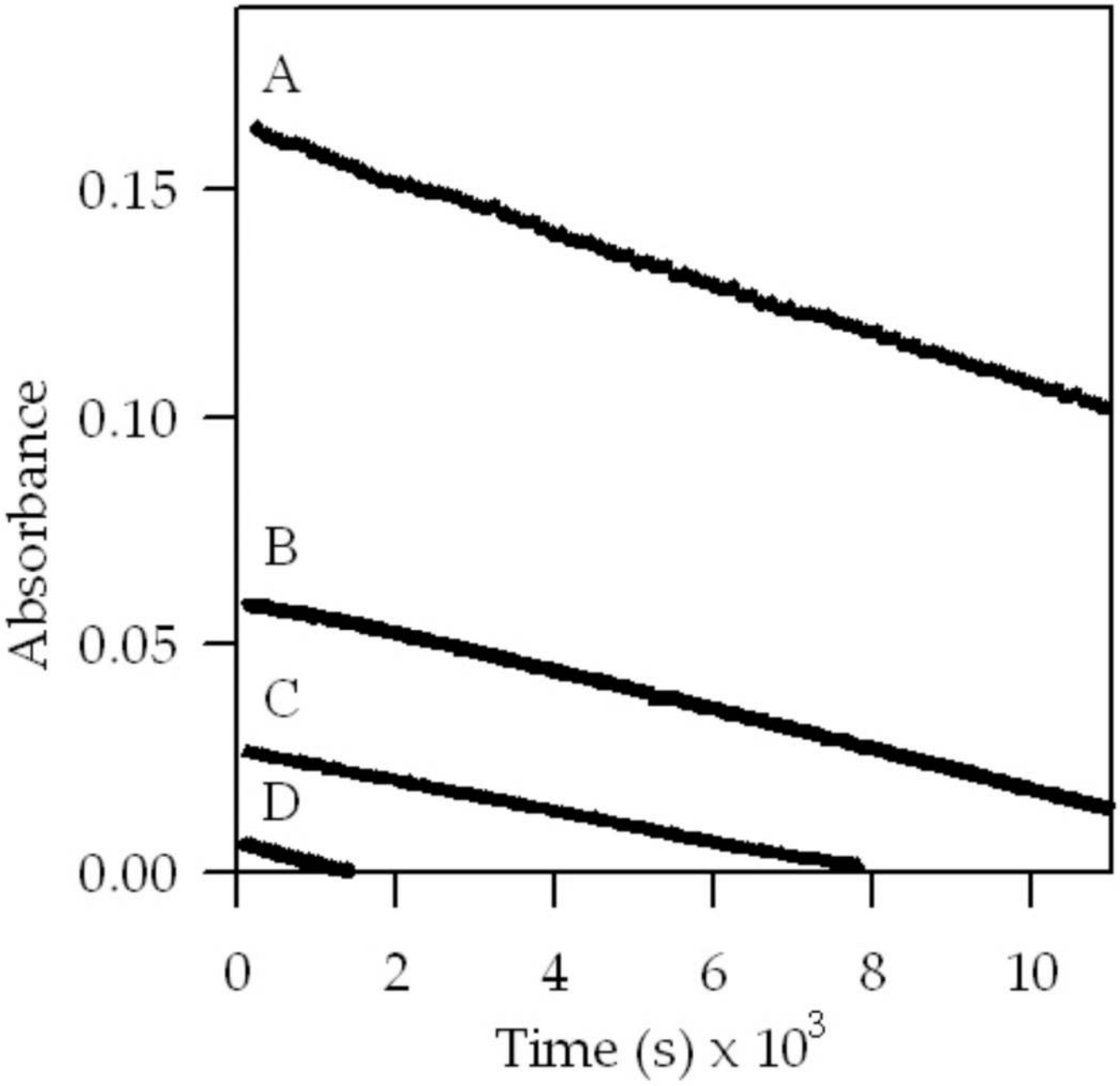

Figure 9.
Plot showing IR absorbance of ester **1** vs time for selected initial concentrations of **1**: (A) 0.10 M; (B) 0.050 M; (C) 0.025 M; (D) 0.004 M.

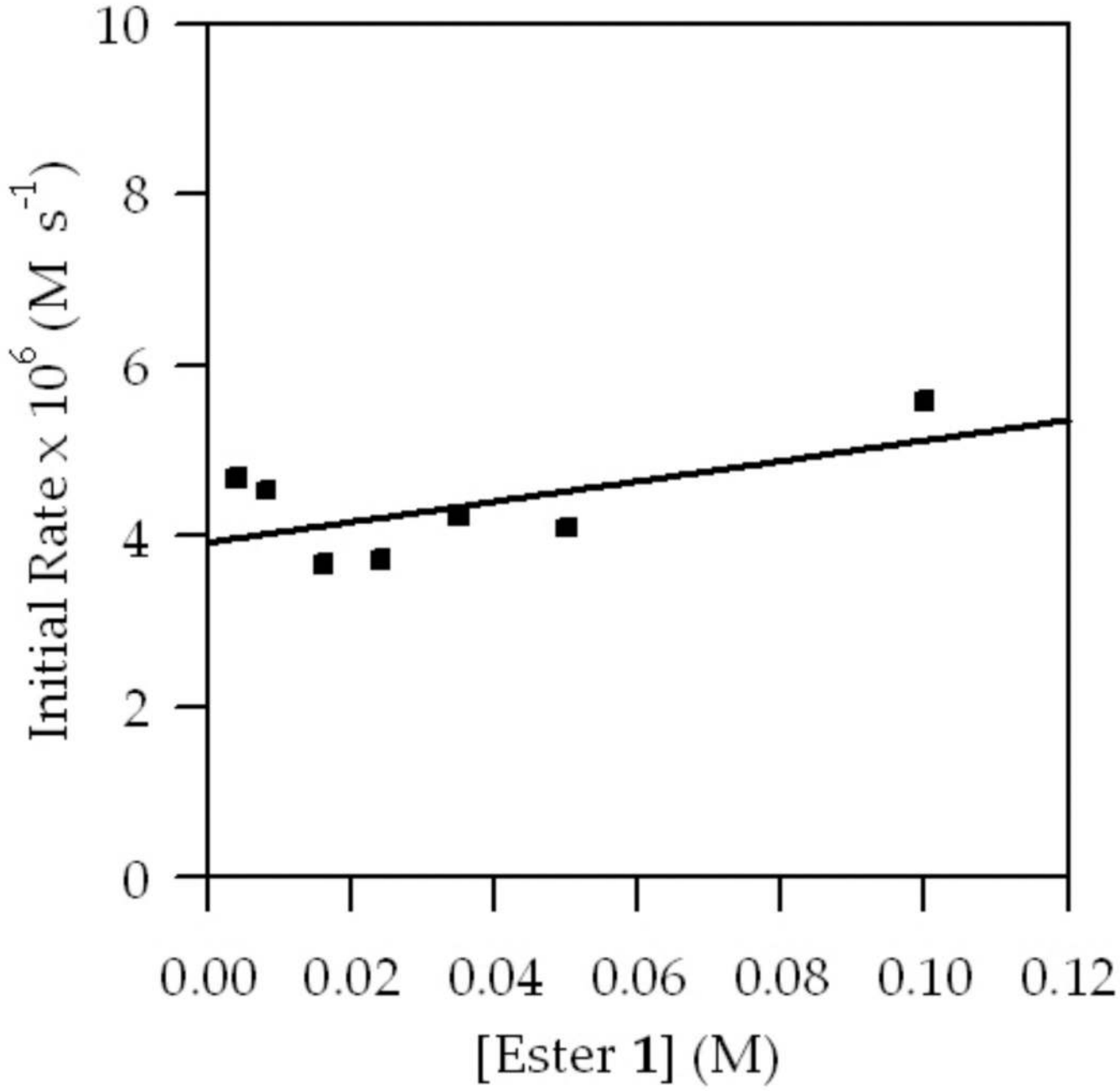

Figure 10.
Plot of slopes vs [substrate] in THF (6.1 M) for the 1,4-addition of ester **1** with LDA (0.10 M) at −78 °C. The curve depicts an unweighted least-squares fit to y = k[ester **1**] + k' (k = (1.2 ± 1) × 10^{-5}, k' = (3.9 ± 0.4) × 10^{-6}).

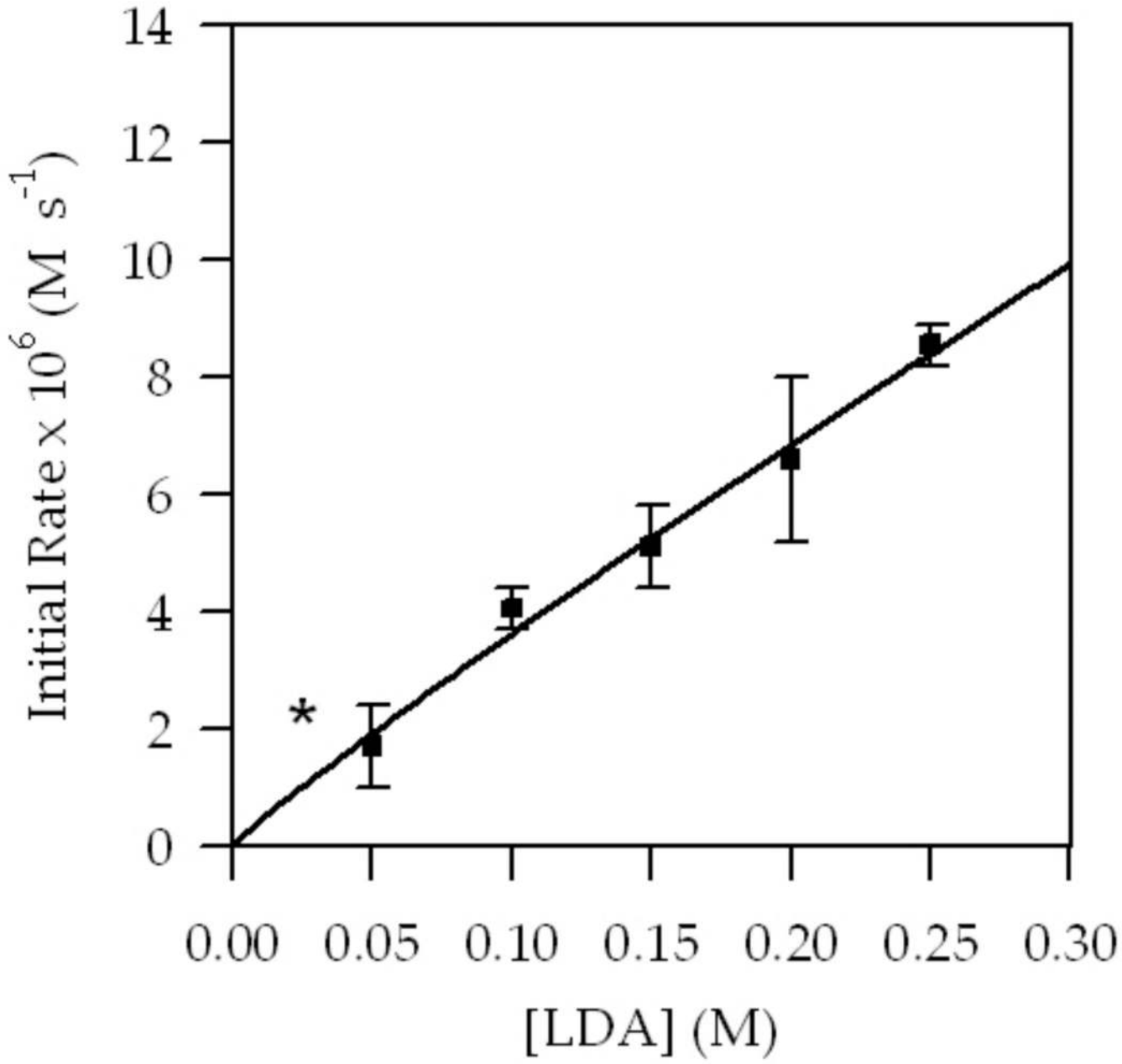

Figure 11.
Plot of initial slopes vs [LDA] in THF (6.10 M) for 1,4-addition of ester **1** (0.004 M) at −78 °C. The curve depicts an unweighted least-squares fit to y = k[LDA]^n (k = (3.1 ± 0.4) × 10^{-6}, n = 0.92 ± 0.03).

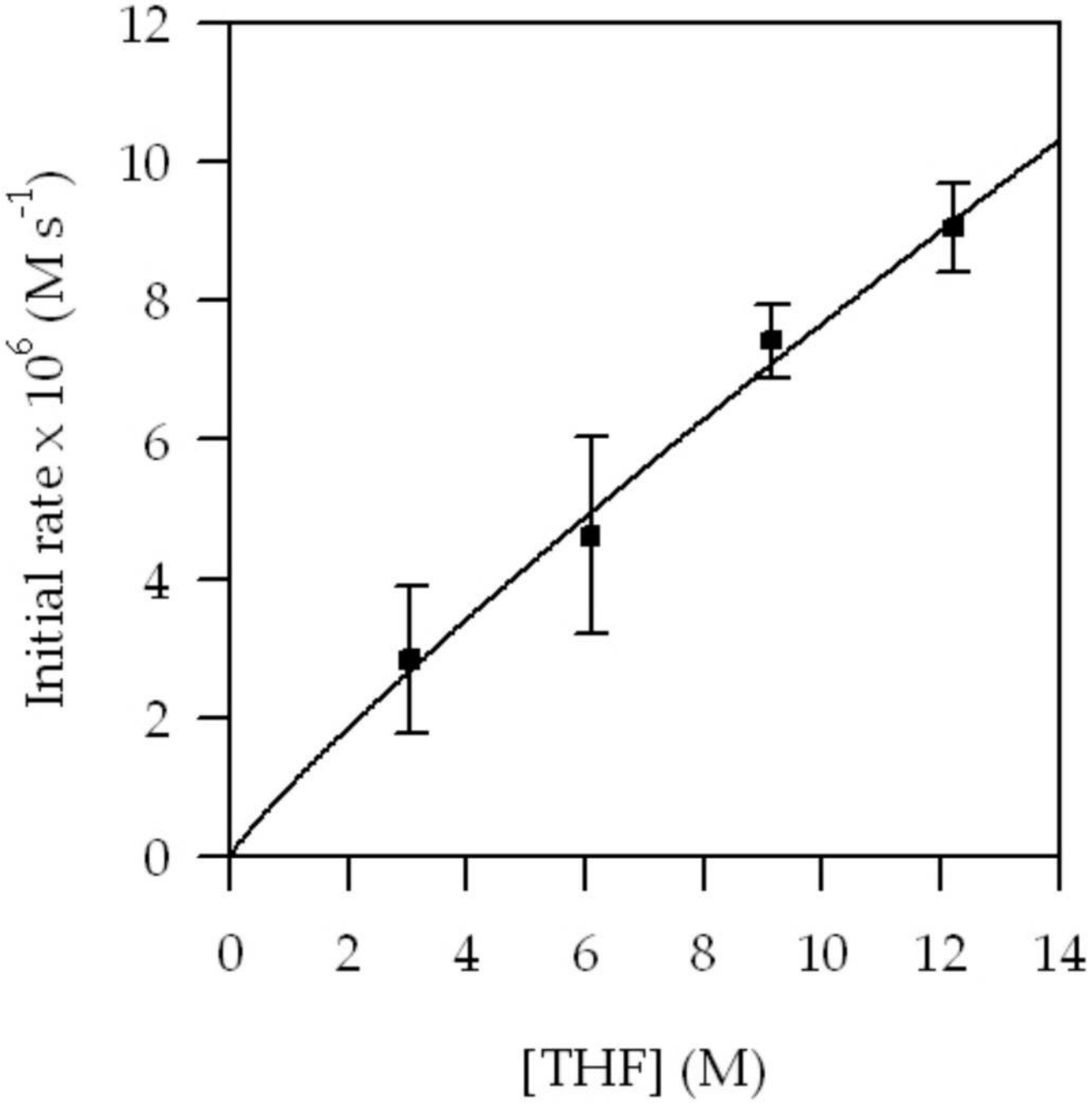

Figure 12.

Plot of initial slopes vs [THF] in hexane cosolvent for 1,4-addition of ester **1** (0.004 M) with LDA (0.10 M) at −78 °C. The curve depicts an unweighted least squares fit to $y = k[\mathrm{THF}]^n + k'$ ($k = (8.1 \pm 0.2) \times 10^{-7}$, $n = 0.95 \pm 0.03$), $k' = (4.05 \pm 0.04) \times 10^{-7}$).

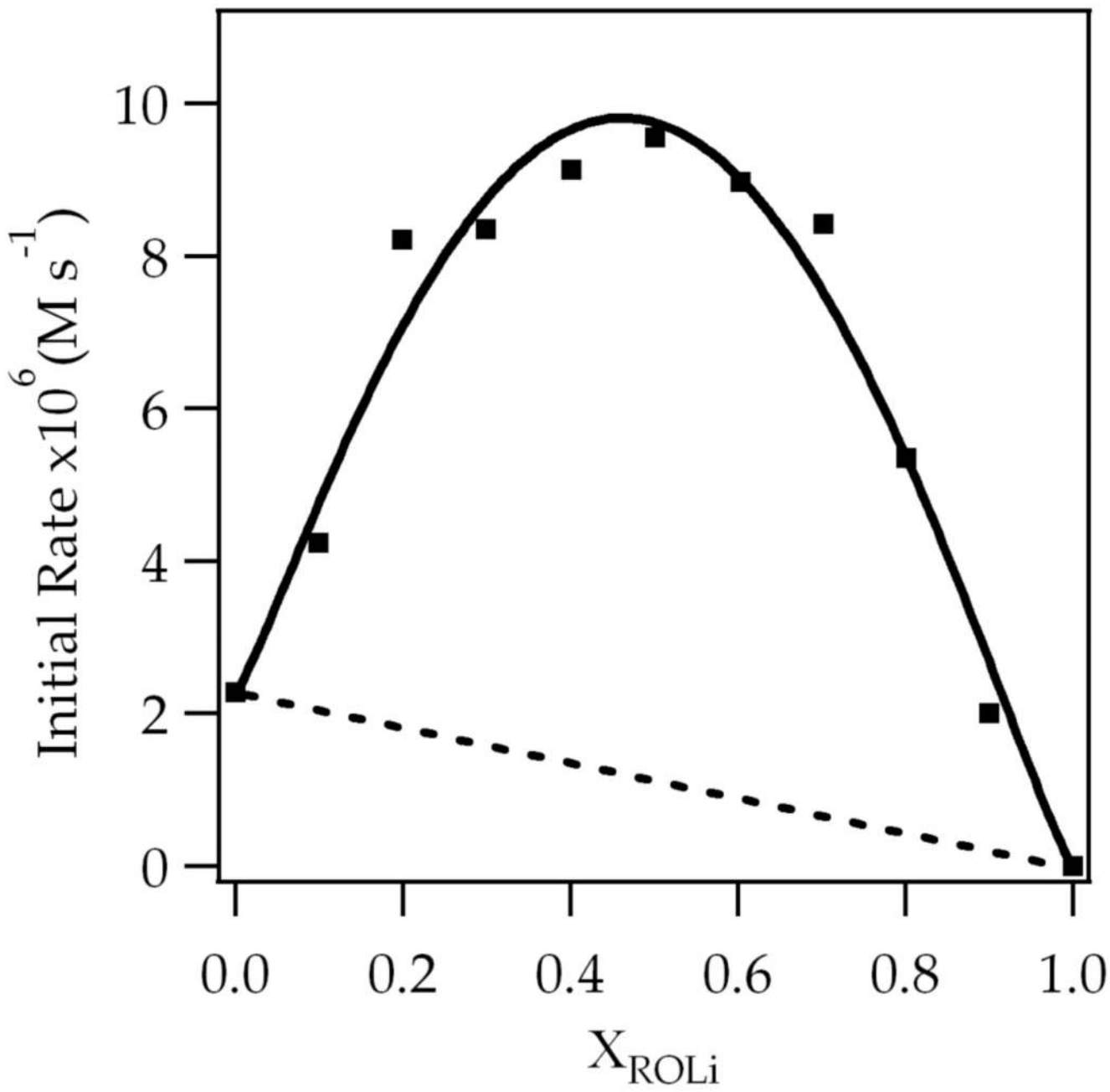

Figure 13.
Plot of initial rate versus mole fraction of enolate (X_{ROLi}) for the serial injection of ten aliquots of ester **1** (10 mol % each relative to LDA) to 0.10 M LDA in 6.1 M THF/hexane cosolvent at −78 °C. The dashed line depicts the theoretical initial rates in the absence of autocatalysis, and the curve represents a non-linear least squares fit to eq 4.

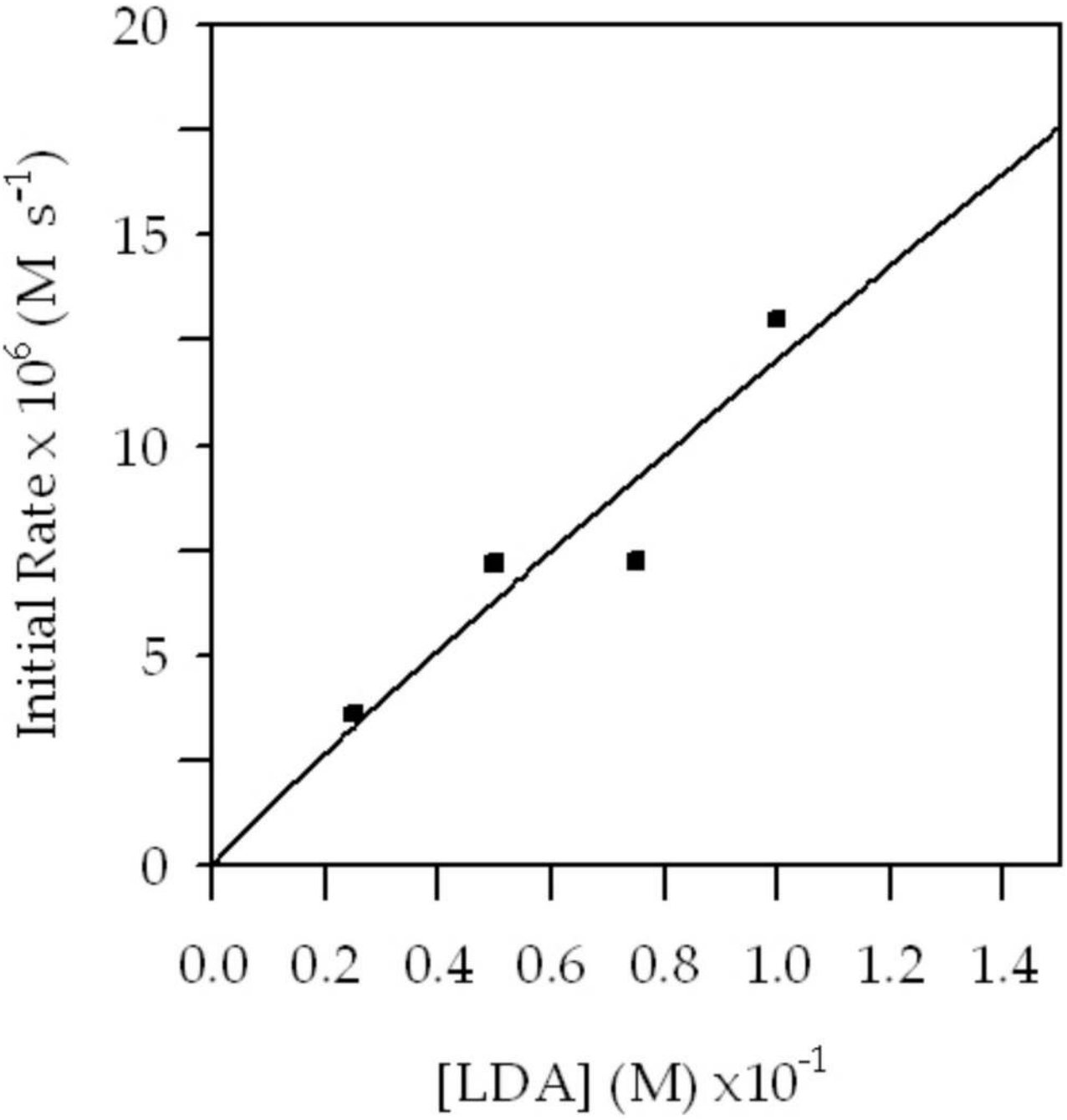

Figure 14.
Plot of initial slopes vs [LDA] for the condensation of LDA dimer **3** (0.10 M) with enolate dimer **5a** (0.025M) in THF (6.10 M) at −78 °C. The curve depicts an unweighted least-squares fit to $y = k[\mathrm{LDA}]^n$ ($k = (1.0 \pm 0.3) \times 10^{-4}$, $n = 0.93 \pm 0.24$).

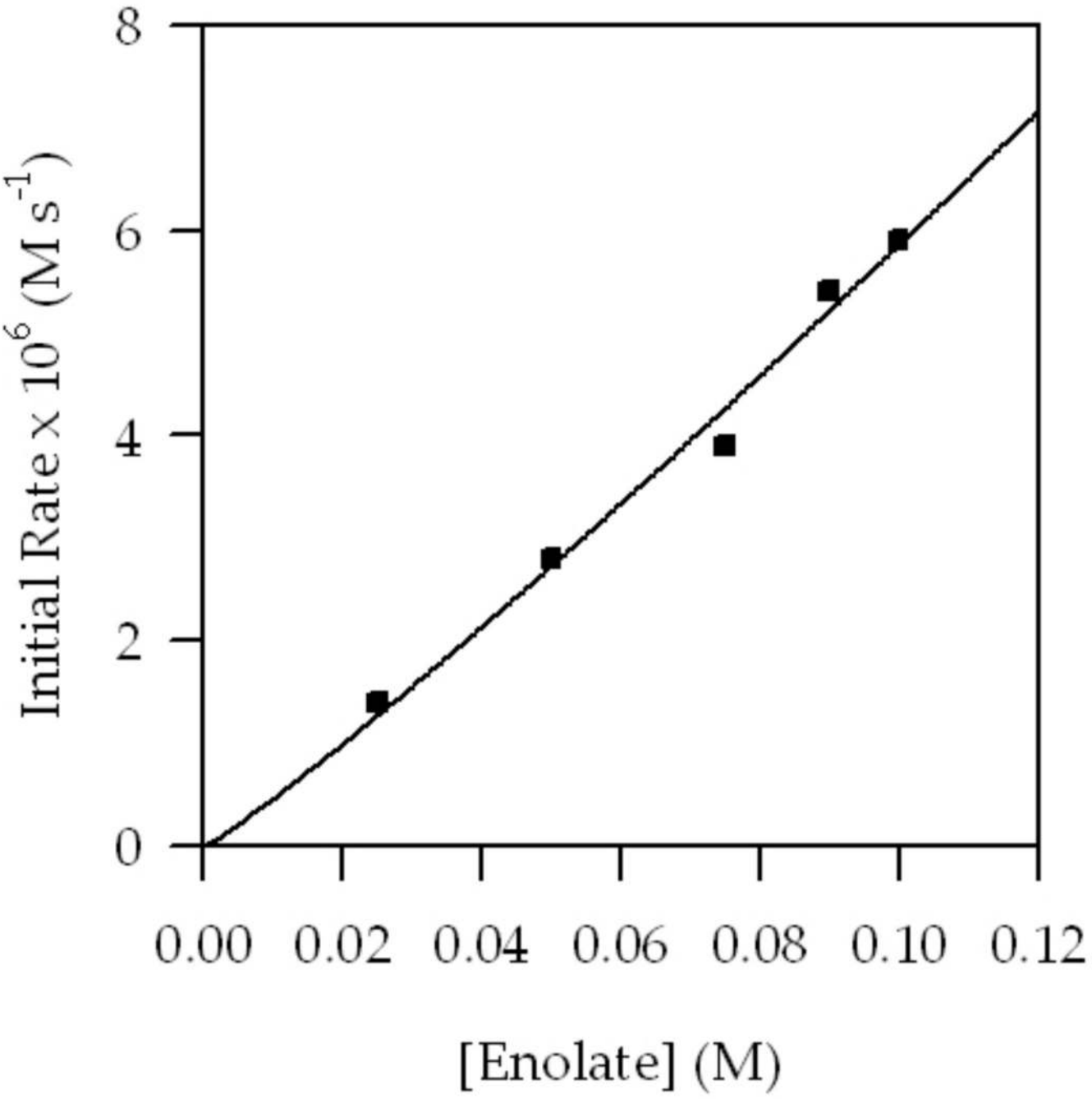

Figure 15.
Plot of initial slopes vs the concentration of enolate **5** for the condensation of LDA dimer **3** (0.10 M) with enolate dimer **5a** (0.025M) in THF (6.10 M) at −78 °C. The curve depicts an unweighted least-squares fit to y = k[enolate]^n (k = (7.4 ± 0.3) × 10^{-5}, n = 1.10 ± 0.14).

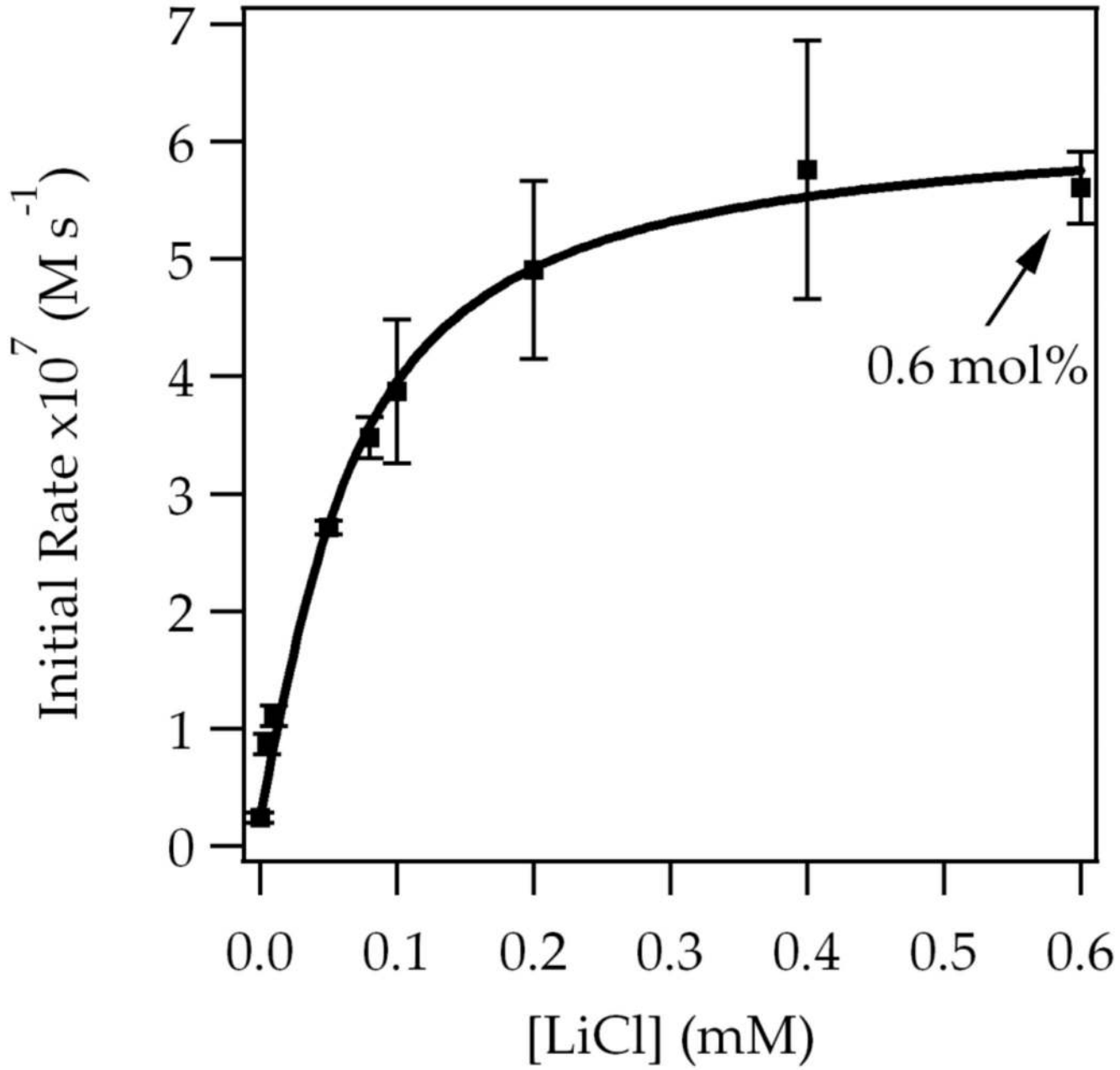

Figure 16.
Plot of initial rates vs [LiCl] in THF (6.1 M) for 1,4-addition of ester **1** (0.004 M) with LDA (0.10 M) at −78 °C. The 0.6 mol % notation is relative to LDA concentration.

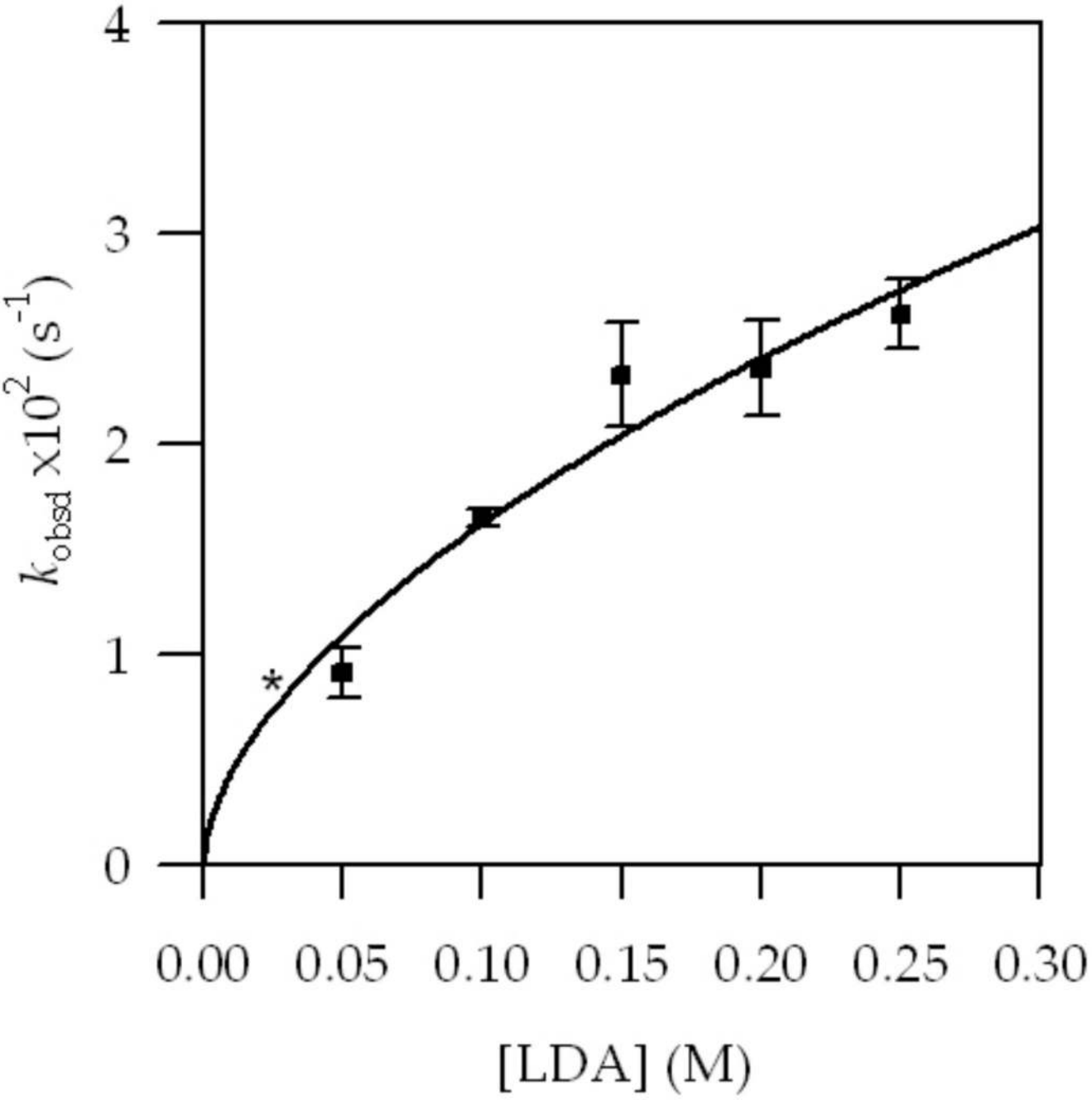

Figure 17.

Plot of k_{obsd} vs [LDA] in THF (6.10 M) for 1,4-addition of ester **1** (0.004 M) in the presence of 1 mol % LiCl at −78 °C. The curve depicts an unweighted least-squares fit to y = k[LDA]^n (k = (6.01 ± 0.04) × 10^{-7}, n = 0.57 ± 0.08). The asterisk denotes a point that departs markedly from pseudo-first-order conditions and is not included in the fit.

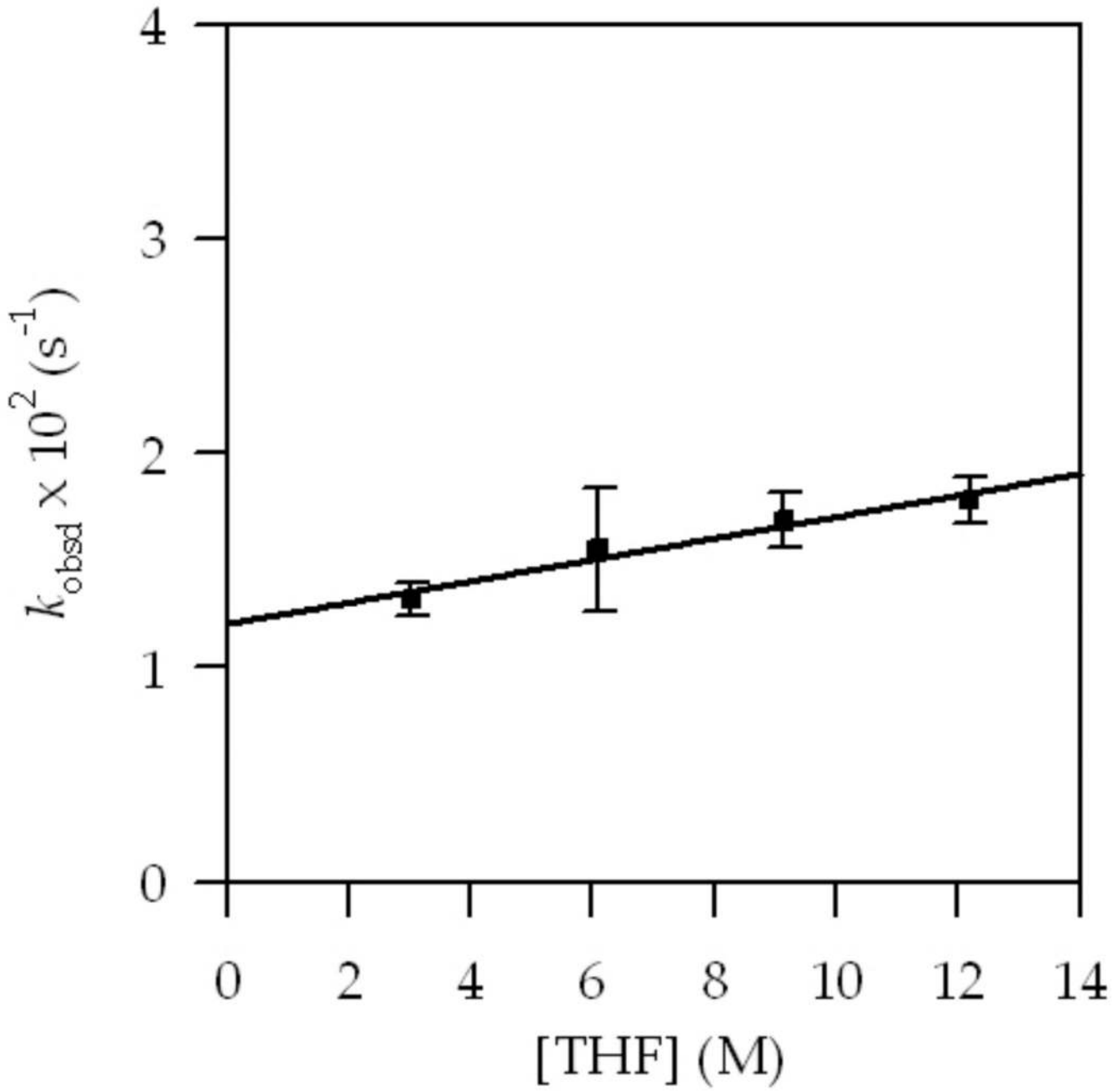

Figure 18.

Plot of k_{obsd} vs [THF] in hexane cosolvent for the 1,4-addition of ester **1** (0.004 M) with LDA (0.10 M) in the presence of 1 mol % LiCl at −78 °C. The curve depicts an unweighted least-squares fit to y = $-k$[THF] + k' (k = (5.0 ± 0.01) × 10^{-4}, k' = (1.2 ± 0.1) × 10^{-2}).

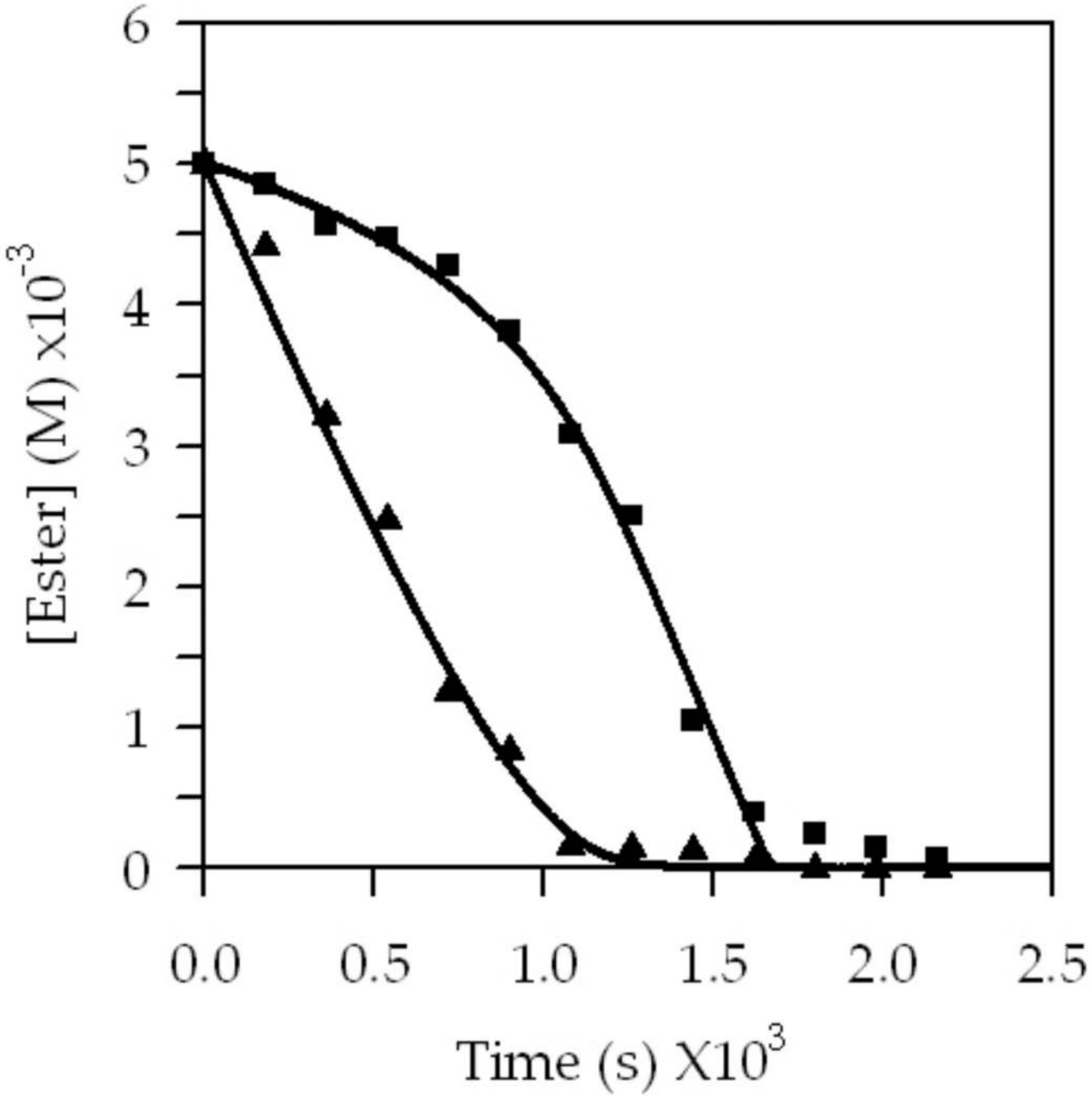

Figure 19.
Plot of ester concentration vs time for the uncatalyzed 1,4-addition of LDA (0.10 M) to a mixture of esters **1** and **12** (0.005 M each) in THF (6.10 M) at −78 °C. Results are analyzed by GC relative to a decane internal standard. (■) Ester **1**; (▲) Ester **12**.

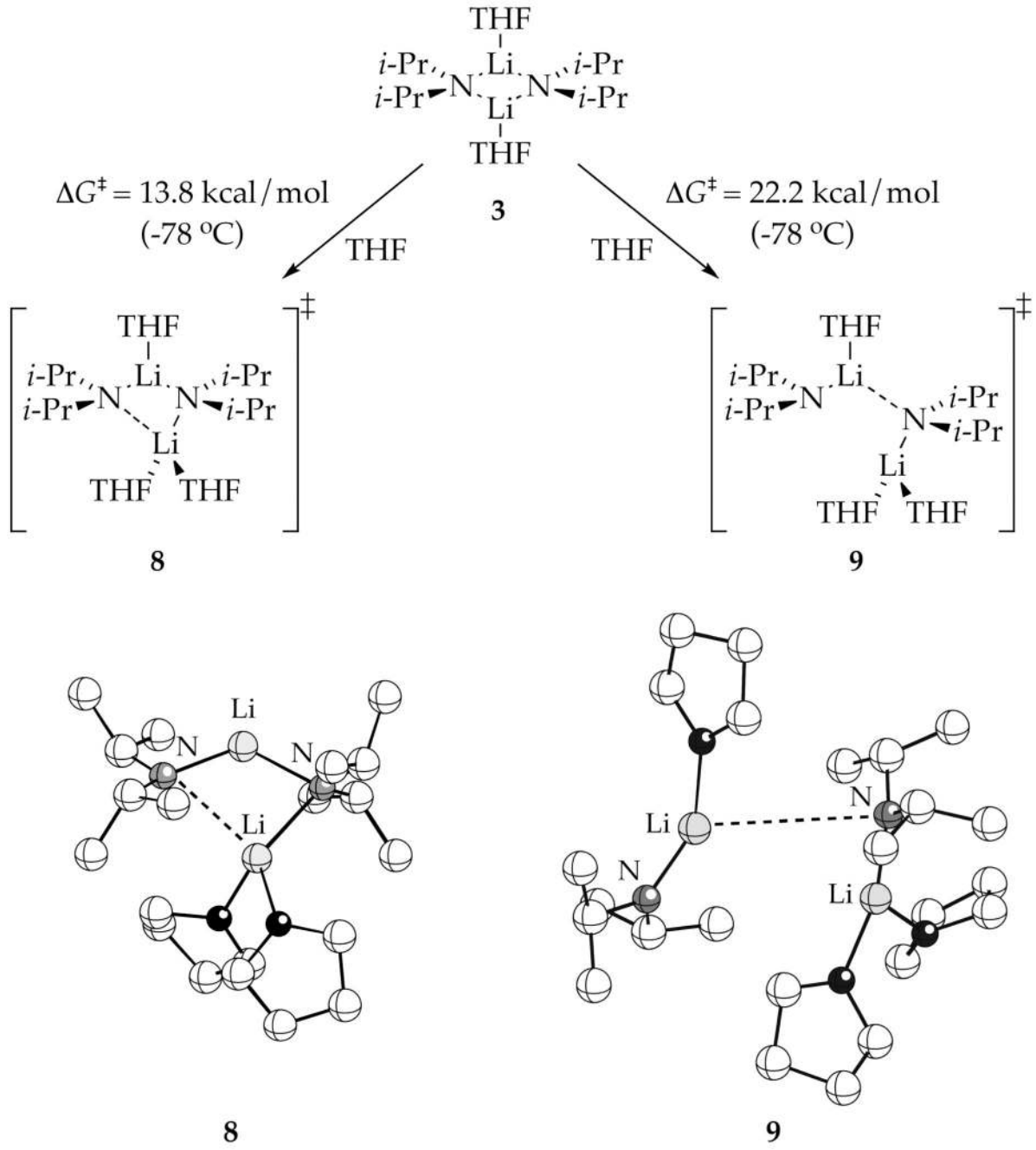

Scheme 1.

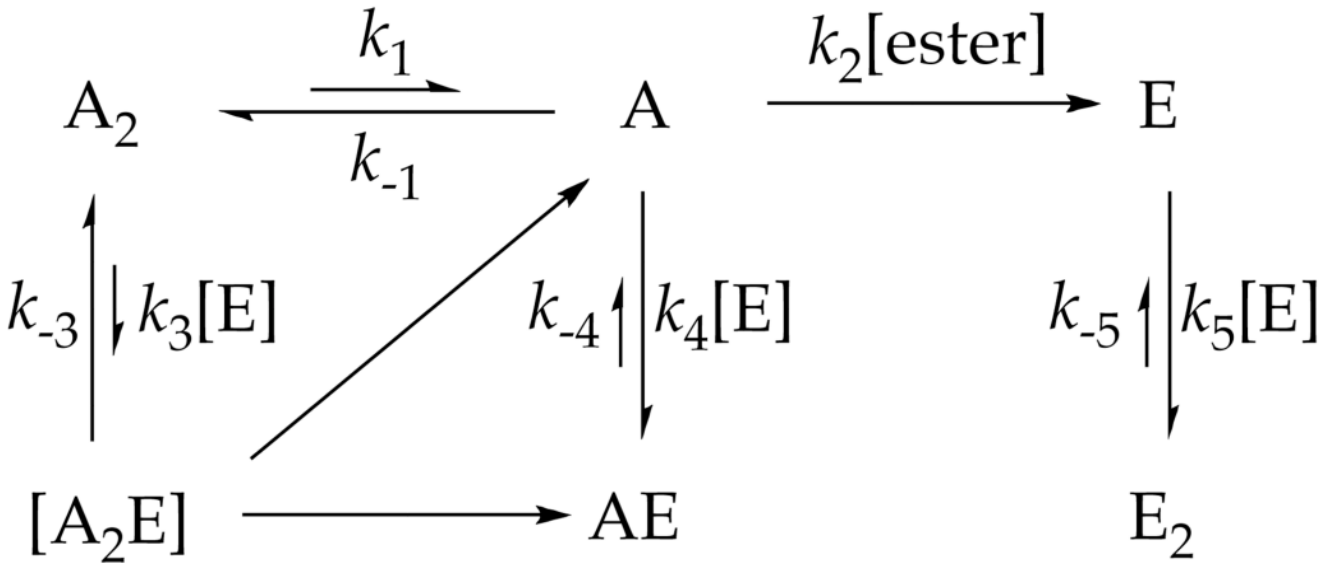

Scheme 2.

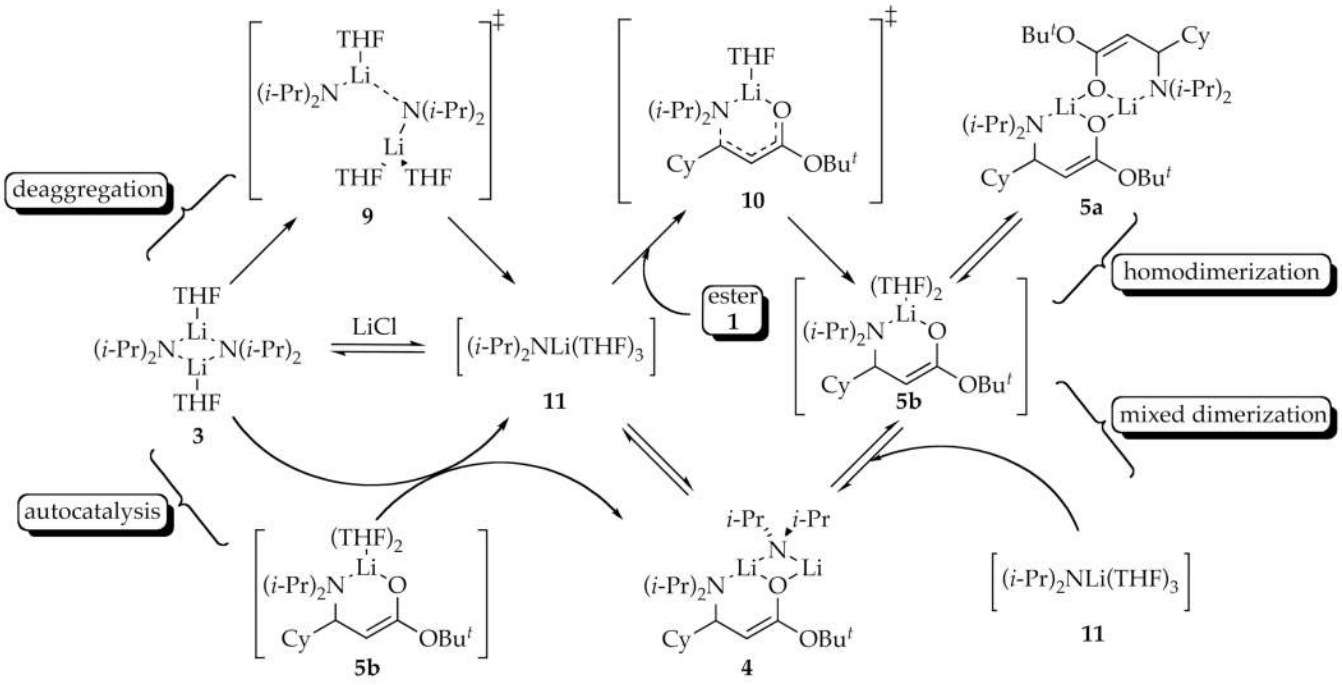

Scheme 3.